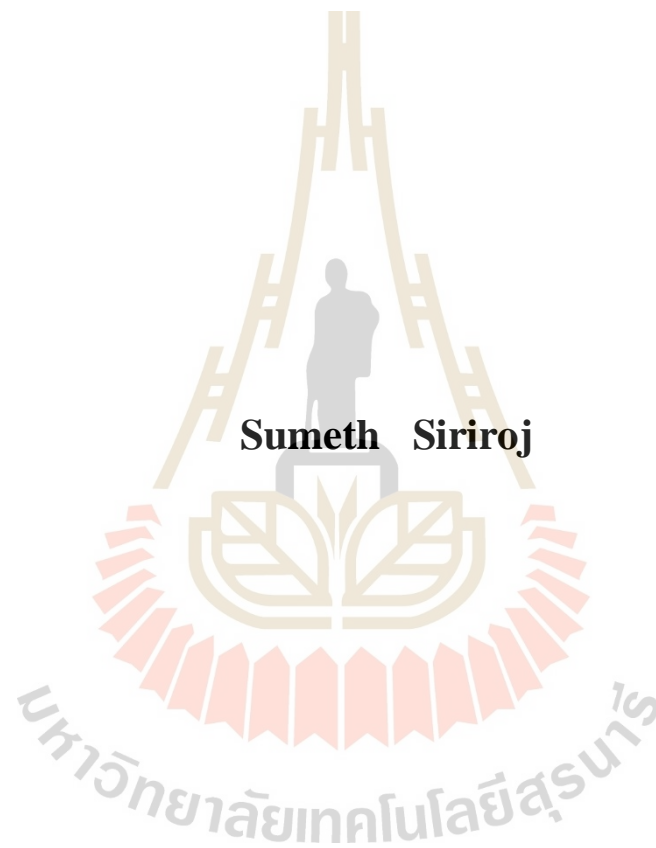


**DIAMONDOID COUNTER ELECTRODES FOR DYE-
SENSITIZED SOLAR CELLS**



**A Thesis Submitted in Partial Fulfillment of the Requirement for the
Degree of Doctor of Philosophy in Physics
Suranaree University of Technology
Academic Year 2017**

ข้อไฟฟ้าจากไดมอนด์อยด์สำหรับเซลล์แสงอาทิตย์ชนิดสีย้อมไวแสง



วิทยานิพนธ์เล่มนี้เป็นส่วนหนึ่งของการศึกษาตามหลักสูตรปริญญาวิทยาศาสตรดุษฎีบัณฑิต

สาขาวิชาฟิสิกส์

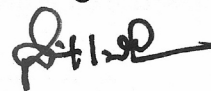
มหาวิทยาลัยเทคโนโลยีสุรนารี

ปีการศึกษา 2560

DIAMONDOID COUNTER ELECTRODES FOR DYE-SENSITIZED SOLAR CELLS

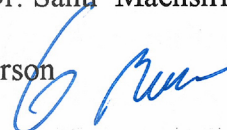
Suranaree University of Technology has approved this thesis submitted in partial fulfillment of the requirements for the Degree of Doctor of Philosophy.

Thesis Examining Committee



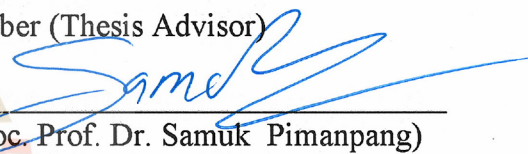
(Prof. Dr. Santi Maensiri)

Chairperson



(Assoc. Prof. Dr. Worawat Meevasana)

Member (Thesis Advisor)



(Assoc. Prof. Dr. Samuk Pimanpang)

Member



(Asst. Prof. Dr. Wirat Jarernboon)

Member



(Assoc. Prof. Dr. Puangratana Pairor)

Member



(Assoc. Prof. Flt. Lt. Dr. Kontorn Chamniprasart) (Assoc. Prof. Dr. Worawat Meevasana)

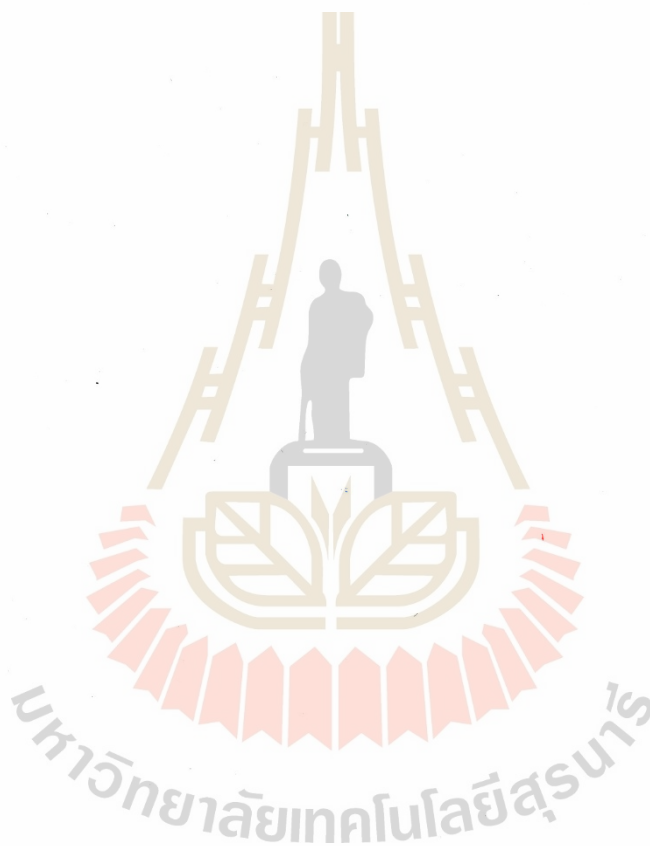
Vice Rector for Academic Affairs
and Internationalization

Dean of Institute of Science

สุเมธ ศิริวรรณ : ขั้วไฟฟ้าจากไดมอนคอยด์สำหรับเซลล์แสงอาทิตย์ชนิดสีข้อมไวแสง
(DIAMONDOID COUNTER ELECTRODES FOR DYE-SENSITIZED SOLAR
CELLS) อาจารย์ที่ปรึกษา : รองศาสตราจารย์ ดร.วรวัฒน์ มีวาสนา, 81 หน้า.

เซลล์แสงอาทิตย์ชนิดสีข้อมไวแสง เป็นทางเลือกใหม่ที่จะทดแทนเซลล์แสงอาทิตย์แบบซิลิกอนและแบบฟิล์มบางที่มีจำหน่ายในปัจจุบัน เนื่องจากเซลล์แสงอาทิตย์ชนิดสีข้อมไวแสงนี้สามารถผลิตได้ง่ายไม่ต้องใช้เทคโนโลยีขั้นสูงและมีราคาถูกกว่าชนิดอื่น สามารถทำให้โปร่งใสได้ อีกทั้งยังมีน้ำหนักเบาอย่างมาก จึงเหมาะในการใช้งานได้อย่างหลากหลาย อย่างไรก็ตามปัญหาใหญ่ที่ทำให้เซลล์แสงอาทิตย์ชนิดนี้ยังไม่ถูกใช้อย่างแพร่หลายนั้นก็เพราะประสิทธิภาพในการเปลี่ยนพลังงานแสงเป็นพลังงานไฟฟ้าที่ได้นั้นยังต่ำเมื่อเทียบกับเซลล์แสงอาทิตย์จากซิลิกอน ซึ่งโดยปกติหากใช้ขั้วไฟฟ้าที่ผลิตจากโลหะแพลทินัมเป็นขั้วเคาท์เตอร์จะให้ความเสถียรสูงและยังให้ประสิทธิภาพที่ดีที่สุด แต่ก็ทำได้สูงสุดแค่เพียงครึ่งเดียวของเซลล์แสงอาทิตย์แบบซิลิกอน ดังนั้นจึงมีความจำเป็นอย่างยิ่งในการพัฒนาขั้วไฟฟ้าให้มีประสิทธิภาพที่ดีขึ้น ในงานวิจัยนี้นำขั้วไฟฟ้าไดมอนคอยด์ ซึ่งเป็นคาร์บอนในโครงสร้างเพชรระดับนาโนเมตรและสามารถสังเคราะห์หรือสกัดได้ง่ายจากของเสียจากปิโตรเลียม มาทำเป็นขั้วเคาท์เตอร์ในเซลล์แสงอาทิตย์ชนิดสีข้อมไวแสง ด้วยวิธีเคลือบด้วยตัวเอง (Self-assembled monolayers technique) ลงบนขั้วไฟฟ้าทองคำ และพบว่าขั้วไฟฟ้าจากไดมอนคอยด์โมเลกุลเล็ก (Adamantane) ให้ประสิทธิภาพเทียบเท่าขั้วไฟฟ้าจากแพลทินัม ยิ่งกว่านั้นขั้วไฟฟ้าจากไดมอนคอยด์โมเลกุลใหญ่ (Tetramantane) ยังให้ค่ากระแสที่สูงมาก ส่งผลให้ได้ประสิทธิภาพสูงกว่าขั้วแพลทินัมถึงร้อยละ 28 การเพิ่มขึ้นของประสิทธิภาพที่ได้นั้นเกิดจากการเพิ่มขึ้นของความหนาแน่นกระแสลัดวงจร (short-circuit current density) ที่สูงมากถึง 27 mA/cm^2 ซึ่งคาดว่าเป็นผลมาจากความสามารถในปรับค่า work function บนขั้วโลหะของไดมอนคอยด์ ทั้งนี้เนื่องมาจากไอโอไดน์อิเล็กโทรไลต์ที่ใช้ในระบบเซลล์แสงอาทิตย์ชนิดนี้ทำปฏิกิริยารุนแรงกับโลหะทองคำ ทำให้เซลล์แสงอาทิตย์ที่ได้ไม่เสถียร และถูกทำลายอย่างรวดเร็ว แนวทางการแก้ปัญหาในงานนี้เลือกเปลี่ยนวัสดุรองรับจากทองคำเป็นโลหะแพลทินัมโดยการปรับปรุงผิวสัมผัสของแพลทินัมด้วยกรดก่อนจะเคลือบไดมอนคอยด์ลงไป และพบว่าสามารถใช้เป็นขั้วสำหรับเซลล์แสงอาทิตย์ชนิดสีข้อมไวแสงที่มีความเสถียรสูง และเพิ่มประสิทธิภาพจากขั้วแพลทินัมเดิมได้ถึงร้อยละ 11 อีกแนวทางที่ถูกใช้ทดสอบคือ การเคลือบฟิล์มไดมอนคอยด์ลงบนซิลิกอนด้วยเทคนิคการเคลือบด้วยไอระเหย (Chemical vapor deposition technique) ซึ่งได้ค่ากระแสในเซลล์แสงอาทิตย์ที่สูงเช่นเดียวกัน แต่มีประสิทธิภาพที่ต่ำกว่าขั้วโลหะแพลทินัม อันเนื่องมาจากความต้านทานไฟฟ้าที่สูงกว่าส่งผลให้ค่า fill factor ลดลง ทั้งนี้เซลล์ดังกล่าวมีความเสถียรสูง

มาก จากข้อดีที่ได้สังเกตพบของข้าวโดมอนด์คอยด์ทำให้สามารถคาดหวังที่จะใช้งานโดมอนด์คอยด์ในงานส่วนอื่น ๆ ที่เกี่ยวข้องกันได้ เช่น ใช้ในกระบวนการเร่งปฏิกิริยาทางแสง ใช้ในตัวเก็บประจุยิ่งยวด หรือใช้ในเซลล์แสงอาทิตย์ชนิดเพอร์รอฟสไกต์ ซึ่งเป็นการเปิดเส้นทางในการสร้างเทคโนโลยีใหม่ๆ ต่อไป



สาขาวิชาฟิสิกส์
ปีการศึกษา 2560

ลายมือชื่อนักศึกษา สุวิมล สิริวงค์
ลายมือชื่ออาจารย์ที่ปรึกษา อ. นพ.

SUMETH SIRIROJ : DIAMONDOID COUNTER ELECTRODES FOR

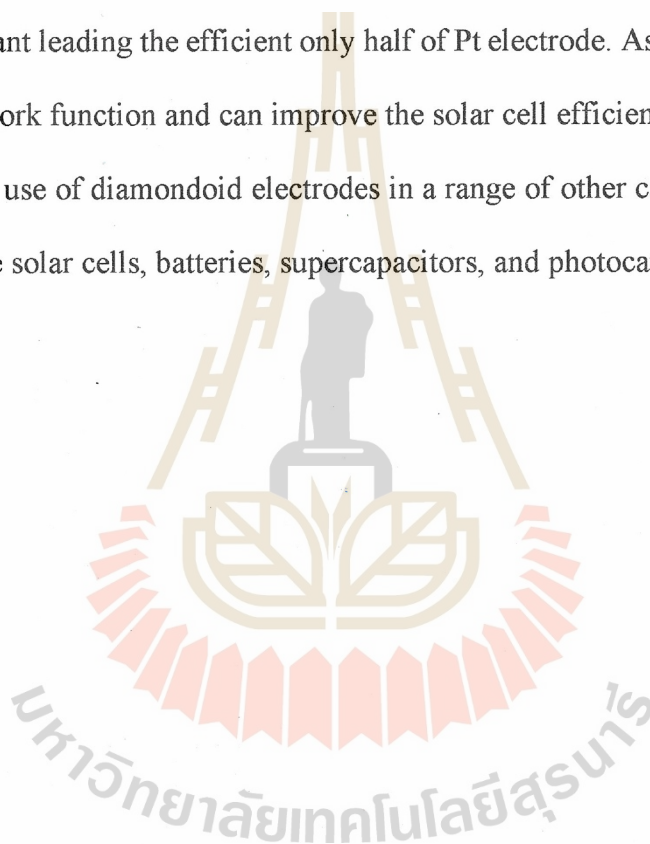
DYE-SENSITIZED SOLAR CELLS. THESIS ADVISOR : ASSOC.

PROF. WORAWAT MEEVASANA, Ph.D. 81 PP.

DIAMONDOID/ADAMANTANE/[121]TETRAMANTANE/DYE-SENSITIZED
SOLAR CELLS (DSSCs)/COUNTER ELECTRODE

Dye-sensitized solar cells (DSSCs) are an alternative type of solar cells which provide much benefit, comparing to commercial silicon or thin film solar cell e.g. low-cost in production, easy to fabricate (no requirement of high technology), transparency, and lighter. However, DSSCs are still not widely in use because the efficiency is still lower than commercial silicon solar cell. The highest recording efficiency of DSSCs is only half of a commercial silicon solar cell. Normally, the best electrode of DSSCs are made from platinum. It is necessary to look for a new type of electrode which could give higher efficiency. Here, we show that counter electrodes of our DSSCs can be made from diamondoids (nanometer-size diamond-like molecules which can be synthesized cheaply or extracted from petroleum waste) and the efficiency can be maintained or improved. When the counter electrodes are made of adamantane (smallest member of diamondoid) on a gold substrate, the power conversion efficiencies are already comparable to Pt electrodes. Then, when the larger diamondoids, [121]tetramantane, are used instead, the efficiencies can outperform Pt reference by more than 28%. This predominantly results from a superior short-circuit current density of up to 27 mA/cm^2 , which we attribute to an adjustable work function of our diamondoid electrodes. However, iodine electrolyte of DSSCs destroyed the gold

substrates and shortens the cell lifetime greatly. To solve the problem, platinum is then selected as the substrate of diamondoid film. After modifying the surface by piranha solution, diamondoid growth on Pt substrate can improve efficiency about 11% from Pt substrate and maintain good stability. On the other hand, diamondoids coated on a silicon substrate via chemical vapor deposition technique (CVD) counter electrode also provide a good stability and large current density but the lower in fill factor from a higher resistant leading the efficient only half of Pt electrode. As diamondoid films can reduce the work function and can improve the solar cell efficiency, this study suggests the potential use of diamondoid electrodes in a range of other catalytic processes such as perovskite solar cells, batteries, supercapacitors, and photocatalytic cells.

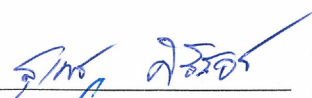


School of Physics

Academic Year 2017

Student's Signature

Advisor's Signature




ACKNOWLEDGEMENTS

I would like to express my sincere thanks to everyone who pushes me to present position. This work could not be completed without the kind support and help from the follow people. First and foremost is my advisor, Assoc. Prof. Dr. Worawat Meevasana. I heard of him long before I joined SUT. from many people during my master's degree at Khon Kane University. He has known as a scientist who is a rising star, who can publish in a very high-ranking journal in the various topic especially about diamondoid and photoemission spectroscopy. After finishing my master's degree, I decided to come forward with him and that changed my life forever. He is very warm, great attitude and always give me new scientific ideas. Not only helping about the thesis, but he also gives me personal counseling and be kind take care my life.

Next person, I also would like to grateful to Prof. Dr. Santi Maensiri, who always pushes me in the right way and a lot of helping especially leading me to know my advisor. He helps me a lot in this work about instrument and materials. He gives me a chance to do new projects such as in energy storage and solar cells project.

I got a chance to study and research abroad at Stanford University, under a supervision of Prof. Zhi-Xun Shen. He is very kind and bring me to see new ideas of top scientists. I also thank Prof. Jeremy Dahl and Prof. Nicholas Melosh in diamondoids group who give the route to explain the mechanism of diamondoids in DSSCs.

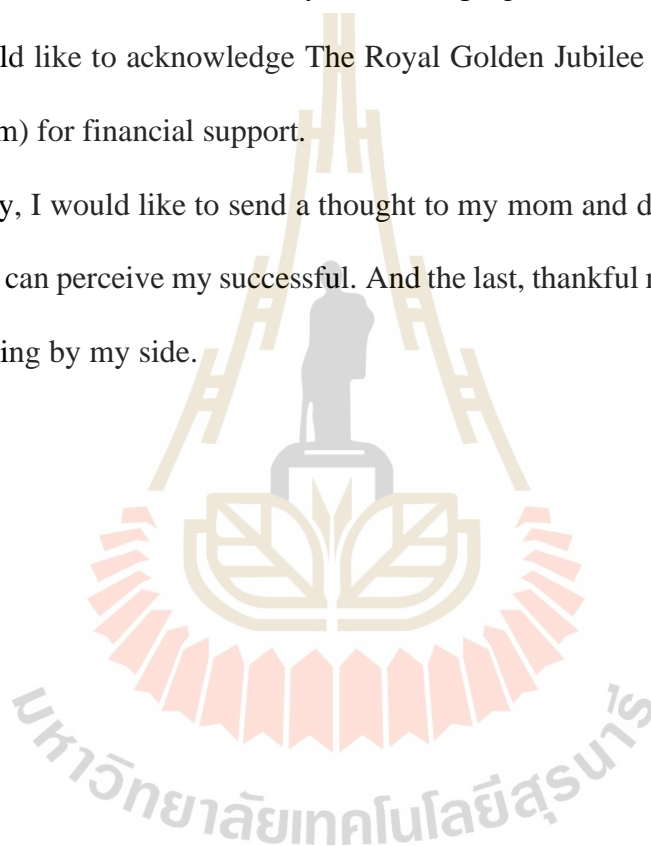
And indispensable, post-doctoral who being as my mentor there, Dr. Hao Yan for sample preparation and platinum surface modifying.

I would like to thank my team in the Meevasana group who support and being here together, especially Mr. Sekson Loapa who help in preparing the working electrode of our solar cell and efficiency measurement. I would like to appreciate teachers and staff in the School of Physics for helping me with everything.

I would like to acknowledge The Royal Golden Jubilee Ph.D. Program (RGJ-Ph.D. Program) for financial support.

Finally, I would like to send a thought to my mom and dad who are in heaven, I believe they can perceive my successful. And the last, thankful my wife Mrs. Sayamol for always being by my side.

Sumeth Siriroj



CONTENTS

	Page
ABSTRACT IN THAI.....	I
ABSTRACT IN ENGLISH	III
ACKNOWLEDGEMENTS	V
CONTENTS.....	VII
LIST OF TABLES	XI
LIST OF FIGURES	XII
LIST OF ABBREVIATIONS.....	XVIII
LIST OF SYMBOLS	XX
CHAPTER	
I INTRODUCTION	1
1.1 Motivation	1
1.2 Diamondoids	3
1.3 Outline of Thesis	7
II BACKGROUND AND LITERATURE REVIEW	9
2.1 A Brief History of Solar Cells	9
2.2 Types of Solar Cells	11
2.2.1 Silicon Solar Cells.....	11
2.2.2 Thin films Solar Cells.....	11
2.2.3 Dye-sensitized Solar Cells.....	12

CONTENTS (Continued)

	Page
2.3 Working Principle of Solar Cells	12
2.3.1 The Sun Spectrum	13
2.3.2 Solar Cells Equivalence Circuit	15
2.4 Dye-Sensitized Solar Cells.....	19
2.4.1 Structure	19
2.4.2 Materials	20
Substrate	20
Scaffold Layer	21
Dye Sensitizer	21
Electrolyte	22
Counter Electrode	22
2.4.3 DSSCs Working Principle.....	23
2.5 History of Diamondoids.....	24
2.6 Electronics Properties of Diamondoids.....	26
2.7 Summary	31
III CONSTRUCTION AND SOLAR CELLS TESTING.....	32
3.1 Material and Instrument Selection.....	32
3.1.1 Material Selection	32
3.1.2 Testing Techniques	33
Solar Simulator	33

CONTENTS (Continued)

	Page
Impedance Analyzer	35
Cyclic Voltammetry	37
Photoemission Spectroscopy	39
Conductive Atomic Force Spectroscopy	40
3.2 Working Electrode Preparation	40
3.2.1 Substrate Cleaning.....	40
3.2.2 Blocking Layer Deposition	41
3.2.3 TiO ₂ Scaffold Layer Coating	41
3.2.4 Dye-Sensitizer Coating	42
3.3 Counter Electrode Preparation	42
3.3.1 Sputter Deposition.....	42
3.3.2 Chemical Vapor Deposition (CVD).....	43
3.3.3 Self-Assembled Monolayers (SAMs)	45
3.4 Electrolyte Preparation.....	45
3.4.1 Iodine Electrolyte Preparation	45
3.4.2 Cobalt Electrolyte Preparation.....	46
3.5 Dye-Sensitized Solar Cells Construction	46
3.6 Summary	47
IV RESULT ANALYSIS AND DISCUSSION.....	48
4.1 Expected Result	48

CONTENTS (Continued)

	Page
4.2 J-V curve and Efficiencies	48
4.2.1 Iodine Electrolyte	48
4.2.2 Cobalt Electrolyte.....	51
4.2.3 CVD Films Counter Electrode.....	54
4.2.4 Platinum Substrate Counter Electrode	55
4.3 Atomic Force Microscopy Result	57
4.4 Impedance Result	59
4.5 Cyclic Voltammetry Result	61
4.6 Photoemission Spectroscopy Result	62
4.6.1 XPS Interpretation of Carbon (C _{1s}).....	62
4.6.2 Work Function	62
4.7 Energy Alignment	64
4.8 Summary	65
V CONCLUSION AND RECOMMENDATION	68
5.1 Conclusions	68
5.2 Recommendation and Future Direction.....	70
APPENDIX	72
REFERENCES.....	75
CURRICULUM VITAE.....	81

LIST OF TABLES

Table	Page
1.1 Experimentally determined optical gaps of diamondoids (Landt, 2010)	7
2.1 The first ionization potentials as measured by photoelectron spectroscopy	29
3.1 ASTM class specifications.....	34
3.2 ASTM spectral irradiance for three standard spectra	35
4.1 Fitting parameter of symmetrical standard models of DSSCs.....	60
4.2 Work function of metals (Tipler and Llewellyn, 1999).....	67

LIST OF FIGURES

Figure	Page
1.1 A schematic diagram of the energy flow in the dye-sensitized solar cells (Postech, Online, 2012)	2
1.2 Schematic diagram of the electron-emission process on diamondoid SAM surfaces. E_F is the Fermi level of the metal substrate, sitting in the energy gap of diamondoid. The vacuum level (E_{vacuum}) is below the conduction-band minimum of the diamondoid, a characteristic of NEA (Yang et al., 2007).....	4
1.3 Diamondoids of different sizes and shapes (Dahl, Liu, and Carlson, 2003). Diamonds are grouped according to their number of crystal cages. The numbers in square brackets indicate the spatial arrangement of the cages according to the Balaban-Schleyer nomenclature. Only the carbon framework is show and the hydrogen surface termination is omitted for clarity (Balaban and Rag Schleyer, 1978)	5
1.4 The C_{1s} core-level spectra of diamondoids (Landt, 2010).....	6
1.5 a) Schematic drawing of the electronic levels of adamantane and adamantane-1-thiol. In the functionalized diamondoid the S electron lone pair gives rise to a thiol state constituting the HOMO of adamantane-1-thiol and, effectively, lowering the gap by 0.6 eV. b) C_{1s} core level spectra for adamantane-1-thiol and adamantane.	

LIST OF FIGURES (Continued)

Figure	Page
<p>Electrons from the C_{1s} core levels are more strongly bounded with the thiol by 0.2 eV. Spectra have been scaled to same height to simplify comparison. (Landt, 2010).....</p>	8
2.1	13
<p>The best efficiency record of solar cells (NREL, 2016).....</p>	13
2.2	14
<p>Black body radiation as a function of wavelength for various absolute temperatures (Miniphysics, Online, 2017)</p>	14
2.3	15
<p>The path length in units of Air Mass, changes with the zenith angle (Newport, Online, 2017).....</p>	15
2.4	16
<p>Standard Solar Spectra for space and terrestrial use (PVEDucation, Online, 2017)</p>	16
2.5	16
<p>Solar cell equivalent circuits including diode inside.....</p>	16
2.6	17
<p>J-V curve of Solar cell (Squirmymcphoe, Online, 2008)</p>	17
2.7	18
<p>Solar cell equivalent circuits with including resistant.....</p>	18
2.8	19
<p>Effect of R_s and R_{sh} to J-V curve a) when R_s is increasing the area of curve was reduce and b) opposition of R_s when R_{sh} decreasing area of curve also decrease</p>	19
2.9	20
<p>Structure of dye-sensitized solar cells (Fraunhofer Institut Solare Energiesysteme, 2011)</p>	20
2.10	22
<p>Structure of N3, N719, black dye and Z-907 sensitizers. (Giribabu, 2012)</p>	22

LIST OF FIGURES (Continued)

Figure	Page
2.11 The schematic diagrams of dye-sensitized solar cells (DSSCs) (Solaronix, Online, 2008)	24
2.12 Adamantane (C ₁₀ H ₁₆) is the smallest closed-cage diamond nanostructure. In a top-down approach it can be constructed by excising a single crystal cell from the bulk diamond lattice (a) and then passivating dangling bonds with hydrogen (b). (Lasse Landt, 2010)	25
2.13 Different diamondoids recrystallized in macroscopic amounts as vander-Waals crystals (Lenzke et al., 2006).....	26
2.14 X-ray absorption spectra of pristine diamondoids (Willey et al., 2005) ..	27
2.15 Valence band photoelectron spectra for a series of diamondoids. The inset shows the determination of the ionization potential (IP) by the interpolation method using the example of [1(2)3] tetramantane. (Landt et al., in preparation)	28
2.16 Schematic diagram of the electron-emission process on diamondoid SAM surfaces. E _F is the Fermi level of the metal substrate, sitting in the energy gap of diamondoid. The vacuum level (E _{vacuum}) is below the conduction-band minimum of the diamondoid, a characteristic of NEA (Yang et al., 2007).....	30
2.17 The reducing of work function from diamondoids (Narasimha et al., 2015).....	30

LIST OF FIGURES (Continued)

Figure	Page
3.1 A graphical representation of the complex impedance plane	36
3.2 Impedance model of DSSCs a) symmetrical setup with c)the impedance model of symmetrical cell and b)real cell setup with d)the impedance model of real cell (G. Yue et al., 2014)	37
3.3 Cyclic voltammetry waveform (M. Timothy, Online, 2006).....	38
3.4 Typical cyclic voltammogram where and show the peak cathodic and anodic current respectively for a reversible reaction. The y-axis shows the negative current (Lifer21, Online, 2005)	38
3.5 XPS system (SLRI, Online, 2016)	39
3.6 Conductive Atomic Force Microscopy (Brukerafmprobes, Online, 2017	40
3.7 Schematics of the sputtering process (R. Pessoa et al., 2014)	43
3.8 Chemical vapor deposition (CVD) system (NaBond Technologies Co., 2017).....	44
3.9 a) The experimental setup of furnace system. b) Evaporation system	44
3.10 The DSSCs fabrication and processes	47
4.1 J-V curve and efficiency of [121]tetramantane-6-thiol on gold substrate (blue) and platinum reference (red) counter electrode	50
4.2 J-V curve and efficiency of adamantane-thiol on gold substrate (black) and platinum reference (red) counter electrode	50
4.3 Decrease of DSSCs efficiency under destroying of iodine electrolyte	51

LIST OF FIGURES (Continued)

Figure	Page
4.4 The DSSCs diagrams (Sugathan, 2015)	52
4.5 Structure of ruthenium-based dye-sensitizer (N719) and porphyrin-based dye-sensitizer (Y123)	52
4.6 J-V curve and efficiency of DSSCs in cobalt electrolyte system	53
4.7 Carbon coated on sapphire substrate a)pristine sapphire and b)after coating with carbon from diamondoid	55
4.8 J-V curve and efficiency of DSSCs from CVD technique	55
4.9 J-V curve and efficiency of [121]tetramantane-6-thiol on platinum substrate (blue) and platinum reference (red) counter electrode	57
4.10 J-V curve and efficiency of adamantane-thiol on platinum substrate (green) and platinum reference (red) counter electrode	57
4.11 AFM images in topography mode of adamantane-thiol/sputtered Au/tungsten substrate a) and sputtered Pt/tungsten substrate b) with roughness (height standard deviation) of 0.40 μm and 0.67 μm , respectively. c) the conductive-mode AFM image of adamantanethiol/Au/W in air with bias = -1 V; the image shows that the electrons can transfer better in the white regions. d) the current vs. voltage curve of adamantane-thiol/Au/W at various points on the sample show the asymmetry between positive and negative bias, indicating that the electrons can transfer out of the substrate better than the other way around	58

LIST OF FIGURES (Continued)

Figure	Page
4.12 The resistive switching behavior shown looping character (Nafe, 2013).....	59
4.13 The result of impedance from Electrochemical Impedance Spectroscopy, point are the raw data and line are fitting curve of insect model	60
4.14 The result of cyclic voltammetry at a scan rate of 20 mV/s in 10mM LiI, 1mM I ₂ , and 0.1M LiClO ₄ in an acetonitrile solution	61
4.15 The result of C1s from the X-ray photoemission (XPS) data of the CVD ada. on Si substrate, measured at SLRI Beamline 3.2a, shows the carbon peaks of both sp ² and sp ³ with the ratio of 81% and 19%, respectively	63
4.16 The work function can be calculated from Einstein relation	63
4.17 The cut off edge of diamondoids on gold and platinum substrate	64
4.18 Energy alignment of DSSCs.....	65
5.1 Schematic of the cation-based model of diamondoids on Au substrate (Narasimha, 2015)	69
A.1 Cut off region from normal materials and from diamondoids.....	73
A.2 The cut off from diamondoid films show the NEA behavior.....	73

LIST OF ABBREVIATIONS

ADA-T/Pt	Adamantane-thiol Coated Platinum
AFM	Atomic Force Microscopy
AM.	Air-mass Coefficient
Au	Gold
CdTe	Cadmium Telluride
Cdl	Double layer capacitance
CIGS	Copper Indium Gallium Diselenide
CNT	Carbon Nano Tube
CV	Cyclic Voltammetry
CVD	Chemical Vapor Deposition
DSSCs	Dye-Sensitized Solar Cells
EIS	Electrical Impedance Spectroscopy
FF	Fill Factor
FTO	Fluorine doped Tin Oxide
GaAs	Gallium Arsenide
GIP	Gallium Indium Phosphide
HOMO	Highest Occupied Molecular Orbitals
HTMs	Hole Transporting Materials
ITO	Indium doped Tin Oxide
J_d	Diode current density
J_{sc}	Short current density

LIST OF ABBREVIATIONS (Continued)

LED	Light-Emitting Diodes
LUMO	Lowest Unoccupied Molecular Orbitals
NEA	Negative Electron Affinity
NREL	The National Renewable Energy Laboratory
PES	Photoelectron Spectroscopy
P_{in}	Sun power on earth ground
Pt	Platinum
PVD	Physical Vapor Deposition
R_{ct}	Charge transfer resistance
R_s	Series resistant
R_{sh}	Shunt resistant
SAMs	Self-Assembled Monolayers
Si	Silicon
TCFs	Transparent Conductive Films
TET-T/Pt	[121] tetramantane-6-thiol coated on platinum
TiO ₂	Titanium dioxide
t_n	Electron lifetime
t_s	Transfer time
V_{oc}	Open circuit voltage
W	Tungsten
XAS	X-Ray Absorption Spectra
XPS	X-Ray Photoemission Spectroscopy
ZnO	Zinc Oxide

LIST OF SYMBOLS

c	Light Velocity
E_F	Fermi energy
E_k	Electron kinetic energy
$P(\lambda)$	Power emitted per unit area per wavelength
ν	Photon Frequency
h	Plank Constant
K	Bozeman Constant
λ	Wavelength
η	Conversion Efficiency
W	Work function
Z	Impedance
ω	Angular Momentum

CHAPTER I

INTRODUCTION

1.1 Motivation

The energy crisis is the main issue for this century because our major energy petroleum-based sources are running out. Alternative energy or renewable energy is the way to solve this problem. Renewable energy includes wind energy, tidal energy, geothermal, biomass and solar energy. The first three sources are geographically dependent and may not be available in many areas. Among these, the solar energy is then the most attractive where the energy power density (per area) can be as high as 1 kW/m² in many parts around the world. Solar energy can commonly be used in two ways: (1) conversion of sunlight to heat, e.g. drying foods/clothes, or heating water and (2) conversion of sunlight to electricity e.g. solar cells or photovoltaic cell. There are three types of solar cell. First is silicon solar cell which is commercially available, but it is relatively very expensive. The second is thin film solar cell which requires advanced technology and creates toxicity. The latest type of solar cell, dye-sensitized solar cell, is relatively cheaper and easier to fabricate; this type of solar cell is expected to play a major role in solving the energy crisis. Dye-sensitized solar cells (DSSCs) was originally co-invented in 1988 by Brian O'Regan and Michael Grätzel in their first published in 1991 (O'Regan and Grätzel, 1991). There are three parts of DSSCs. First, is working electrode with dye molecule as a sensitizer. When electrons in dye molecules absorb photons, they will be excited to exciton state, then transport through the metal

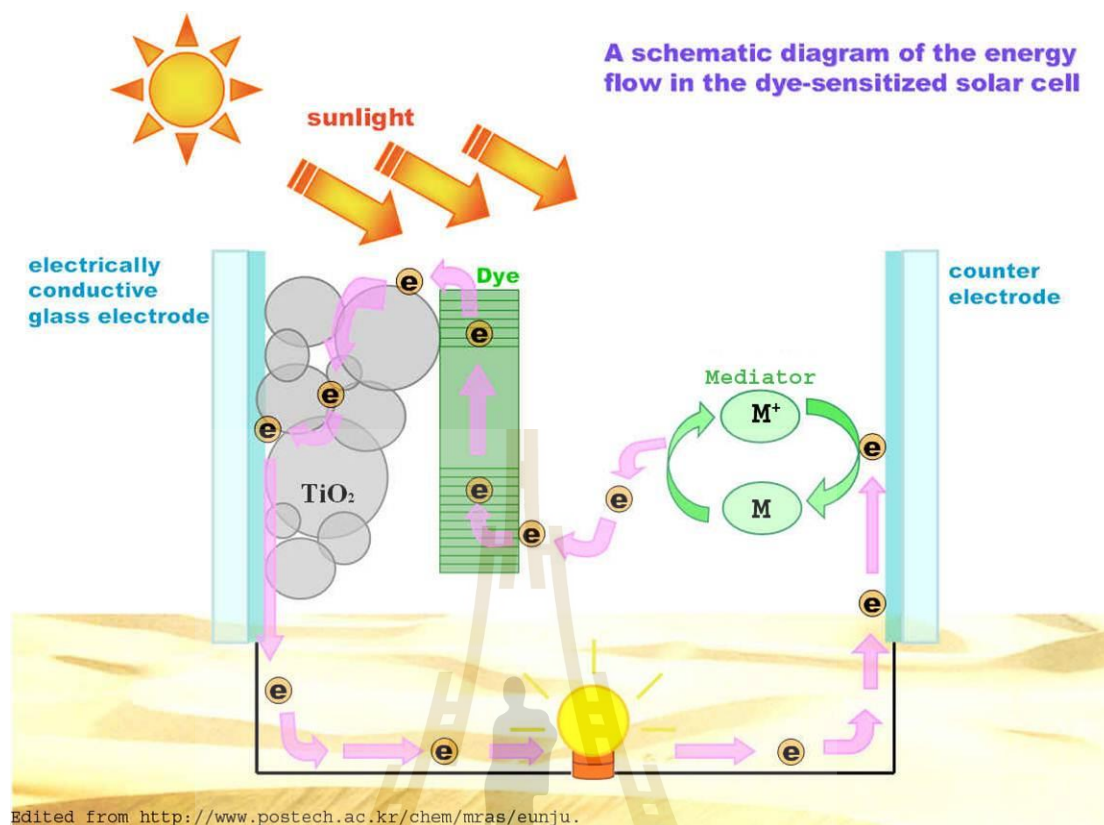


Figure 1.1 A schematic diagram of the energy flow in the dye-sensitized solar cells (Postech, Online, 2012).

oxide layer and load device and then go to counter electrode undergoing the redox reaction of an electrolyte. Generally, platinum (Pt) is recognized as the best counter electrode although it is very expensive. Besides Pt, there are also other materials usable for the counter electrode such as conductive polymer and carbon materials (Imoto et al., 2003). We are interested in the carbon-based materials because carbon is very abundant in the world (Hoover, 2014) and much cheaper than platinum. Carbon film can be coated on conducting glass by various methods: lamination of nano-tube paste (Hwang et al., 2007), spraying of a CNT solution (Lee et al., 2005), a growth of a

precursor or hydrothermal deposition (Siriroj et al., 2012). Chemical vapor deposition (CVD) is one famous method for growing carbon film. Normally, carbon film from CVD uses methane as a precursor (Hernadi et al., 1996). However, in this thesis, we use diamondoid (nano molecule of diamond) as the precursor because diamondoid has negative electron affinity (NEA) (Yang et al., 2007) which may be useful as a counter electrode to return electrons back to the cell (Meevasana et al., 2009). And we also use direct immersing technique or self-assembled monolayers technique with very easy by immersing a gold substrate in diamondoid -thiol solution and leave it overnight. Diamondoids will undergo a self-assembly on the gold substrate (Yang et al., 2007).

1.2 Diamondoids

Diamondoids were classified by the number of crystal cages; the smallest 1-cage structure is called adamantane. The 2-cage structure is called diamantane, the 3-cage structure is called triamantane and so on. These 3 structures are usually called lower diamondoids. The higher diamondoids start from a 4-cage structure because they have different structural isomers. There are four structural isomers for tetramantane where two of them are enantiomers; there are ten different isomers for pentamantane and more than one-hundred isomers for octamantane. Balaban and von Schleyer introduced a method to distinguish these isomers in a nomenclature, including the spatial arrangement of the cages. The name of polymantane is preceded by a number in square brackets that indicates the orientation of the cages along the four axes of a tetrahedron (Balaban and Rag Schleyer, 1978). The X-ray photoemission spectroscopy (XPS) can be used for measuring the C_{1s} core-level of carbon. The common chemical state of binding energy should be at 284 eV for sp^2 - hybridized (pure graphite) and

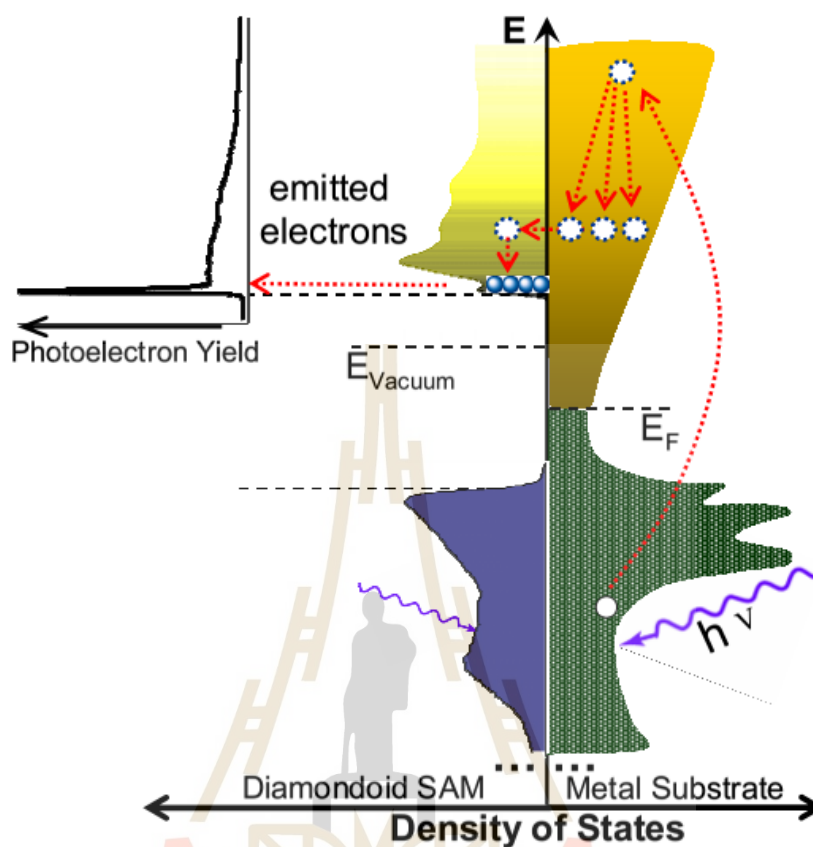


Figure 1.2 Schematic diagram of the electron-emission process on diamondoid SAM surfaces. E_F is the Fermi level of the metal substrate, sitting in the energy gap of diamondoid. The vacuum level (E_{Vacuum}) is below the conduction-band minimum of the diamondoid, a characteristic of NEA (Yang et al., 2007).

284.8 eV for sp^3 - hybridized (pure diamond). Diamondoids are pure sp^3 hybridized form of carbon; C_{1s} energy level will have a smaller shift toward lower binding energies with increasing size of carbon atom (Landt, 2010). The first ionization potential will also have a shift of 9.23 eV for adamantane and of 8.00 eV for hexamantane. These shifts will lead to the change in the optical band gaps as shown in Table 1 (Landt, 2010).

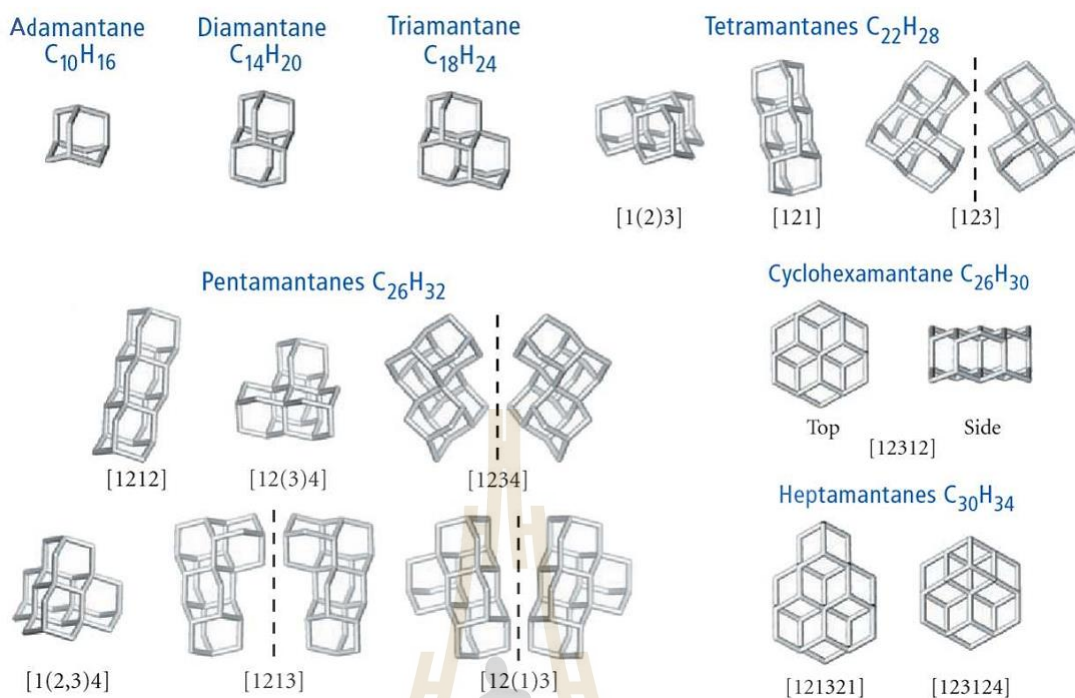


Figure 1.3 Dia

mondoids of different sizes and shapes (Dahl, Liu, and Carlson, 2003). Diamondoids are grouped according to their number of crystal cages. The numbers in square brackets indicate the spatial arrangement of the cages according to the Balaban-Schleyer nomenclature. Only the carbon framework is shown and the hydrogen surface termination is omitted for clarity (Balaban and Rag Schleyer, 1978).

To change the properties of diamondoids, one can modify the structure with a thiol function (i.e. replacing a hydrogen atom in diamondoids by a sulfur atom). This will also shift the C1s to higher binding energies. The lone-pair electron of sulfur gives rise to a thiol state constituting the HOMO of adamantane-1-thiol and lowering the gap by 0.6 eV.

In this thesis, we use adamantane as precursor for CVD technique to mixing sp^2 and sp^3 - hybridized because DSSCs need sp^2 to transfer electron (Velten et al., 2012)

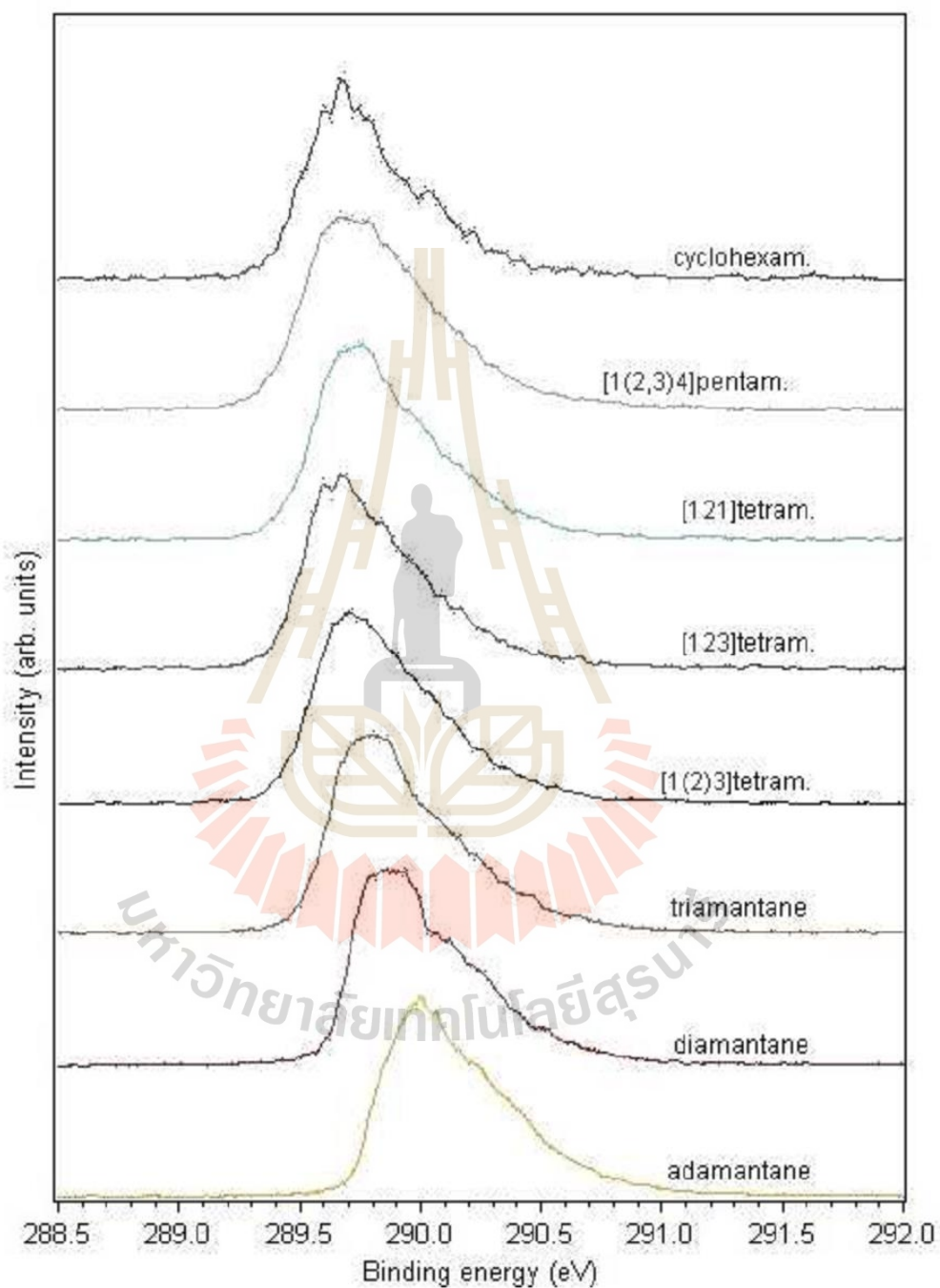


Figure 1.4 The C1s core-level spectra of diamondoids (Landt, 2010).

where negative electron affinity (NEA) of sp^3 may be useful for returning electron back to the cell via the counter electrode. We also use adamantane-1-thiol as the precursor for direct immerse technique on gold substrate for the better electronic properties.

Table 1.1 Experimentally determined optical gaps of diamondoids (Landt, 2010).

Diamondoids name	Optical gap (eV)
adamantane	6.492
diamantane	6.404
triamantane	6.057
[121] tetramantane	6.097
[123] tetramantane	5.953
[1(2)3] tetramantane	5.941
[1212] pentamantane	5.847
[12312] hexamantane	5.881
[1(2,3)4] pentamantane	5.807
[1213] pentamantane	5.787
[12(1)3] pentamantane	5.828

1.3 Outline of Thesis

The thesis is organized as follows. The background of solar cells and diamondoids will be detailing in chapter II, including of a brief history of the solar cell, type of solar cell, the working principle of the solar cell, dye-sensitized solar cell working principle, history of diamondoids and electronic properties of diamondoids. Chapter III will set for describe DSSCs fabrication and cells construction. Including of method and device selection for testing and characterizing materials. Dye-sensitized

solar cells (DSSCs) including of three part, the working electrode, electrolyte, and counter electrode each part preparation were explained in this section. The result of this thesis will explain in chapter IV. The result will explain in term of DSSCs efficiency,

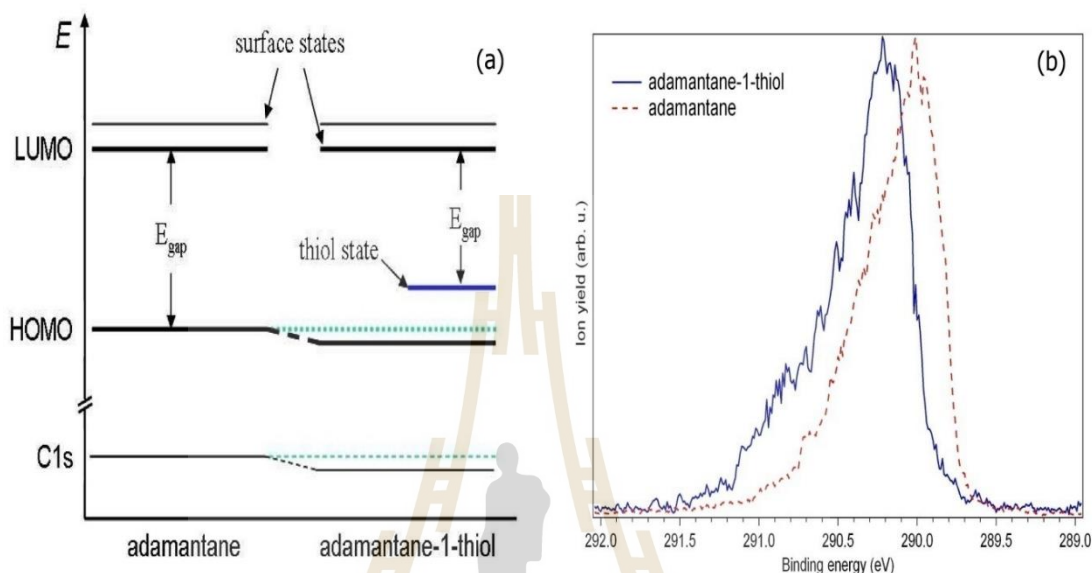


Figure 1.5 a) Schematic drawing of the electronic levels of adamantane and adamantane-1-thiol. In the functionalized diamondoid the S electron lone pair gives rise to a thiol state constituting the HOMO of adamantane-1-thiol and, effectively, lowering the gap by 0.6 eV. b) C1s core level spectra for adamantane-1-thiol and adamantane. Electrons from the C1s core levels are more strongly bounded with the thiol by 0.2 eV. Spectra have been scaled to same height to simplify comparison. (Landt, 2010).

the effect of resistant from impedance result, the redox reaction from CV, electronic properties from PES then energy alignment will conclude the result. And finally, Chapter V will set for summary and concluded the result and future work direction would show.

CHAPTER II

BACKGROUND AND LITERATURE REVIEW

This section was set for detailing the background of solar cells device, including the Sun spectrum and how to manage it to convert into electrical energy, the solar cell principle also considered then focus on diamondoids materials which were used as a precursor of this work.

2.1 A Brief History of Solar Cells

Solar power has been considering for a long time since human history begin. Predecessor uses solar energy to keep self-warming and preserving food. Until 1839, Edmond Becquerel discovered the photovoltaic effect, some materials were created the electrical voltage when irradiate by sunlight. Many years after that Willoughby Smith discovered the photoconductivity of selenium in 1873, selenium has more conductive when it absorbs light this meaning electron in selenium can absorb solar energy and move faster. Then in 1883 Charles Fritts successes to create the first solar cell by coating the thin layer of gold on selenium surface. His solar cells achieved 1% of solar conversion. The photoelectric effect was first observed by Heinrich Hertz in 1887, an electron of solid surface can free by irradiate of Sunlight. Hertz found that electron has more energy when exposed to UV light (the energy of free electron does not depend on the intensity of light) and this effect was explained by Albert Einstein in 1905.

In 1953 Scientist at Bell Laboratories produce silicon solar cell with have more efficient than selenium at 6% of conversion energy. In 1955 Western Electric try to begin selling commercial licenses solar cell technology and Hoffman Electronics Semiconductor creates 2% of efficiency commercial solar cell with cost is about \$1785 / watt. However, in 1958 they can make better cells at 9% conversion and cheaper than before, the government support to use it to power satellite. Because of oil prices rose in the 1970s solar power was developed for alternative energy and successfully to reduce the cost to \$20-\$40 / watt (made from lower grade silicon). The National Renewable Energy Laboratory (NREL) was set by Federal Government of the United States in 1977. Si solar cell has been continuing to develop to increase the efficiency and reduce the cost, however, in 1994, a new type of solar cell was created by using thin films of gallium indium phosphide and gallium arsenide and the efficiency was exceeding to 30% (NREL) At the same time in 1988s, Michael Grätzel and Brian O'Regan Chemists from Germany were invented the dye-sensitized solar cells (DSSCs), a new type of solar cells by using organic dye compound as the sensitizer. The cost of DSSCs is half of Si solar cell and easier to produce. After a few years' development Grätzel was achieved his DSSCs to 11% of solar conversion in 1996. In the early 21st century, solar cell panels became a popular DIY hobby in general because the cost is very low (\$2-\$3/watt). Moreover, DSSCs has been develop by replace dye-sensitizer with perovskite material in 2009 by Miyasaka and called perovskite solar cells (Kojima et al., 2009). In the beginning the efficiency of perovskite solar cell is only 3.8% and has been improved to 22.1% in a single junction world record efficiency in 2016 by Korea University of Science and Technology.

2.2 Types of Solar Cells

As mention in the previous part, there are many types of solar cell, it is beginning with selenium to silicon solar cell then develop to thin films solar cell and the new type is the dye-sensitized solar cell with has been developing to perovskite in finally. This part was set to descript each type of these solar cells.

2.2.1 Silicon Solar Cells

Silicon solar cell is most popular and more than 80% of the commercial solar cell is Si solar cell. Because of highly efficient conversion (15%-20%) with module panel, longevity (company warranties over 20 years), easy to install on ground or roof top and environmentally friendly. However, there are some drawbacks that brake Si solar cell to widely uses. The important reason is Si solar cell is very expensive especially a single crystal silicon solar cell (highest efficiency), the cost is about \$4-\$6 per watt. Although polycrystal and amorphous Si solar cell have been created for replacing the single crystal with cheaper, the efficiency of these cells is also dropped. The other reason is Si solar cell is fragile so it needs a strong frame to hold the cells and this makes Si solar cell heavy until cannot installing on a rooftop.

2.2.2 Thin Films Solar Cells

Although Si solar cell is very high efficiency, to produce Si solar cell is require a very clean process to form a crystal of silicon and it very hard to control. A new type of solar cell, thin films solar cell is lower cost manufacturing process and using fewer materials. There are many types of thin film solar cells such as cadmium telluride (CdTe), gallium indium phosphide (GIP) gallium arsenide (GaAs) and copper indium

gallium diselenide (CIGS), this type is powerful to produce a large-scale product. However, thin films solar cells require very high technology to form thin films under very high vacuum ambient and during the process, it generates some of the toxicity. Moreover, the precursor materials for thin films solar cells are very expensive and not abundant.

2.2.3 Dye-Sensitized Solar Cells

The limiting of above solar cell is it require high technology to produce so this difficult to develop in general. In 1988s Grätzel present a new type of solar cells called Dye-sensitized solar cells (DSSCs). DSSCs imitate photosynthesis of plants, by using an organic dye which can absorb photon energy from sunlight and can be generating electron into conduction state of metal oxide layer then this can use as electric power as well. DSSCs is very easy to produce and do not need any high technology thus it can make and develop from everyone. It uses cheaper materials to fabricate consequently the cost of DSSCs is very lower than Si solar cell (less than \$1/watt). Furthermore, DSSCs is lower weight, can make it transparent and can be flexible with may use in widespread. However, DSSCs has efficient only about a half of Si solar cell and quite low stability, this needs more researcher to improving. The figure 2.1 shown the best efficiency of DSSCs comparing with the other.

2.3 Working Principle of Solar Cells

The solar cell is a device which uses to converting solar energy to electricity, the efficiency of solar cell is relating to Sun spectrum and absorption of solar cell sensitizer.

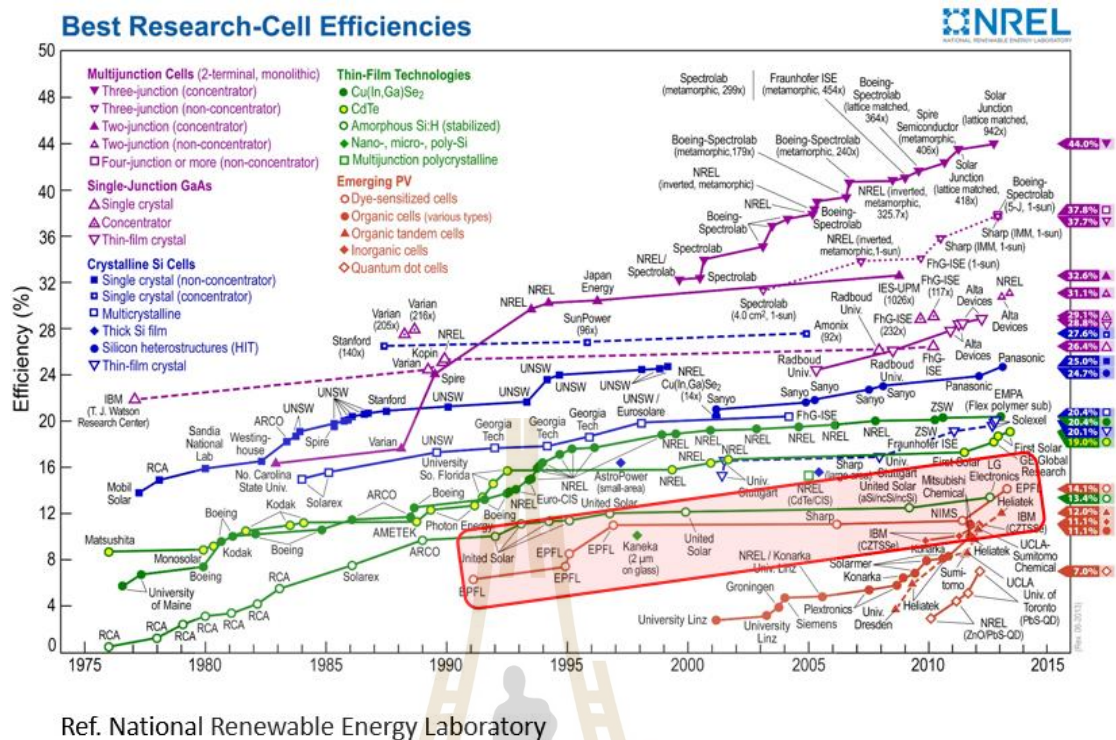


Figure 2.1 The best efficiency record of solar cells (NREL, 2016).

2.3.1 The Sun Spectrum

The temperature of the Sun surface is around 5800K so the spectrum from the Sun looks like from black body at 5800K as following Planck radiation law (Miniphysics, Online, 2017):

$$P(\lambda) = \frac{2\pi hc^2}{\lambda^5 (e^{hc/\lambda \cdot \kappa T} - 1)} \quad (2.1)$$

$P(\lambda)$ is power emitted per unit area per wavelength interval at wavelength. After taking the derivative of this equation, it becomes to Wien displacement law:

$$\lambda_{peak} T = 2.898 * 10^{-3} mK \quad (2.2)$$

The spectrum at various temperature is shown in figure 2.2, as the maximum intensity of solar spectrum is at 500 nm wavelength.

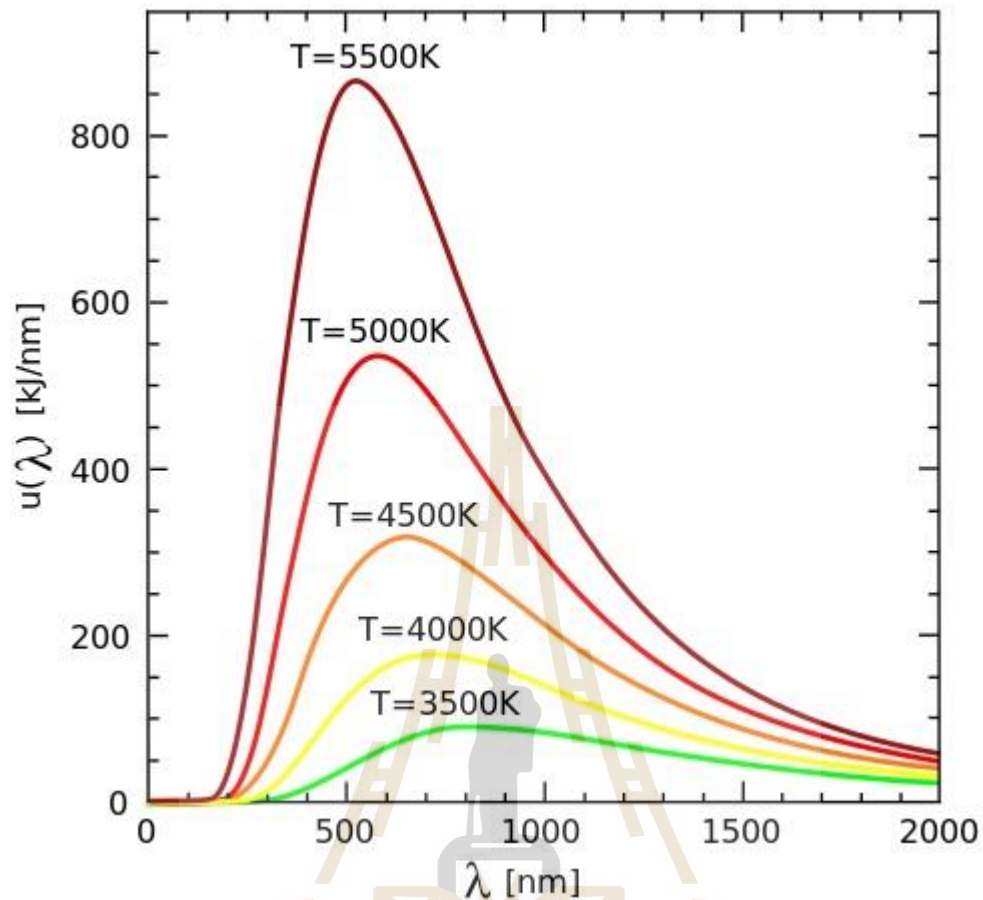


Figure 2.2 Black body radiation as a function of wavelength for various absolute temperatures (Miniphysics, Online, 2017).

However, the correct spectrum on the Earth must concern the absorption of an atmosphere. For the atmosphere with a thickness L_0 , the real part of light through the atmosphere is L equal to $L_0/\cos(\alpha)$, when (α) is an incident angle of light and a normal line of earth. The ratio of L_0/L is defined as Air-mass coefficient (AM.) The standard spectrum for testing the efficiency of solar cell is AM.1.5G with the incident angle of 48 degree and total power density is 1000 W/m^2 , the other air-mass geological as shown in figure 2.3 and its spectrum is shown in figure 2.4.

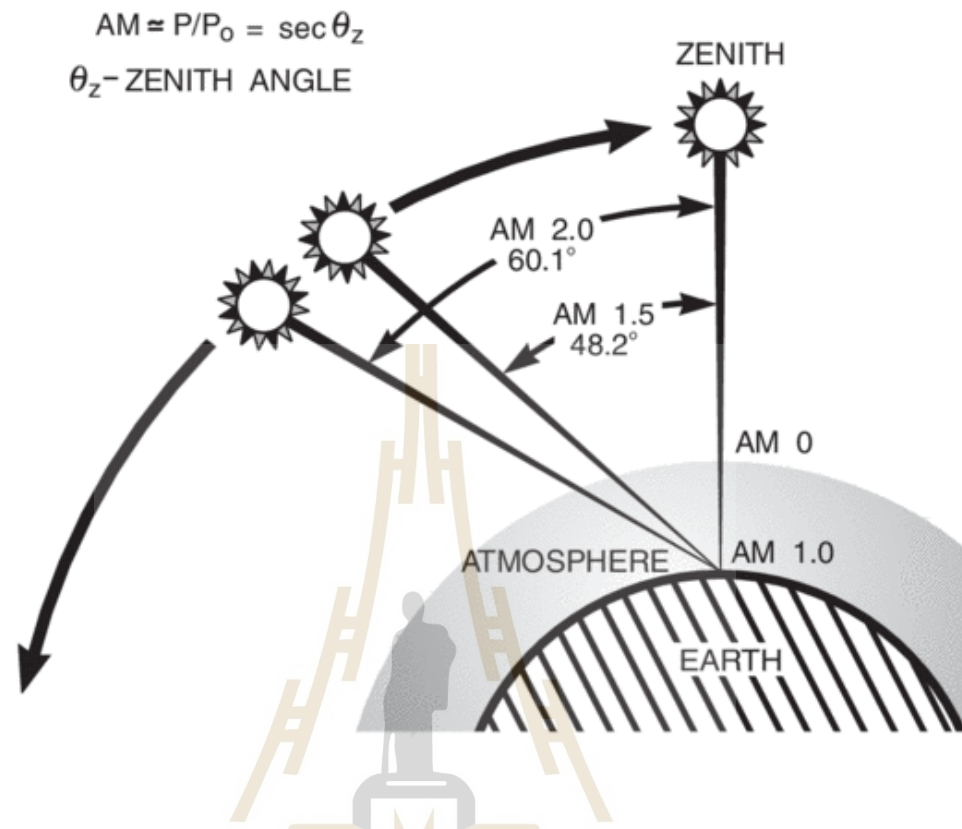


Figure 2.3 The path length in units of Air Mass, changes with the zenith angle (Newport, Online, 2017).

2.3.2 Solar Cells Equivalence Circuit

Solar cells convert solar energy into electrical energy. In general, the solar cell is the P-N junction, thus it behaves as a diode. As solar cell generates the electric current as a battery and a diode connected in parallel. When the light hits the solar cell, electric current will be divided into the diode and an external device as shown in figure 2.5.

The electric current density can be calculated on:

$$J_{sc} = J_d + J \quad \text{or} \quad J = J_{sc} - J_d \quad (2.3)$$

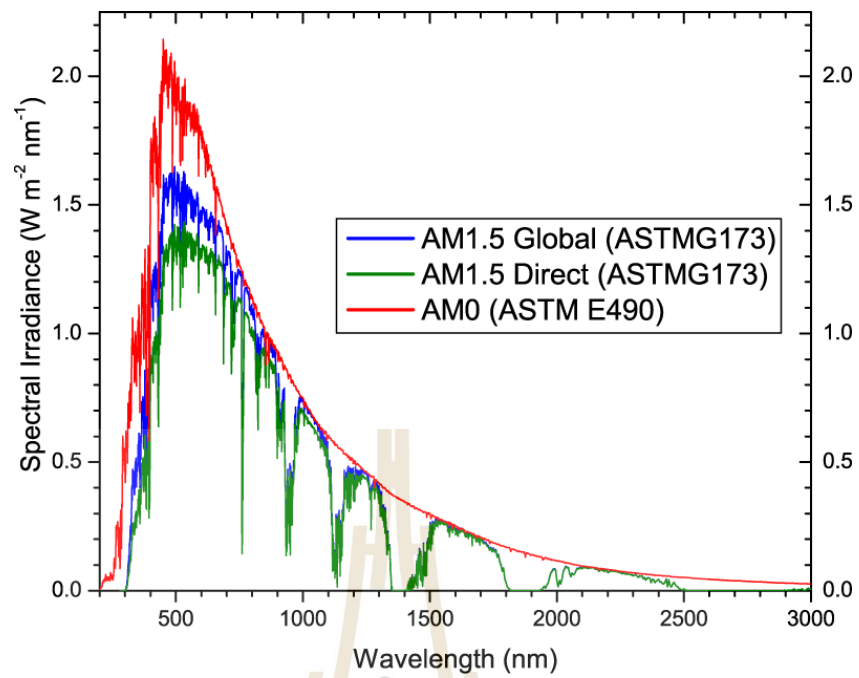


Figure 2.4 Standard Solar Spectra for space and terrestrial use (PVEDucation, Online, 2017).

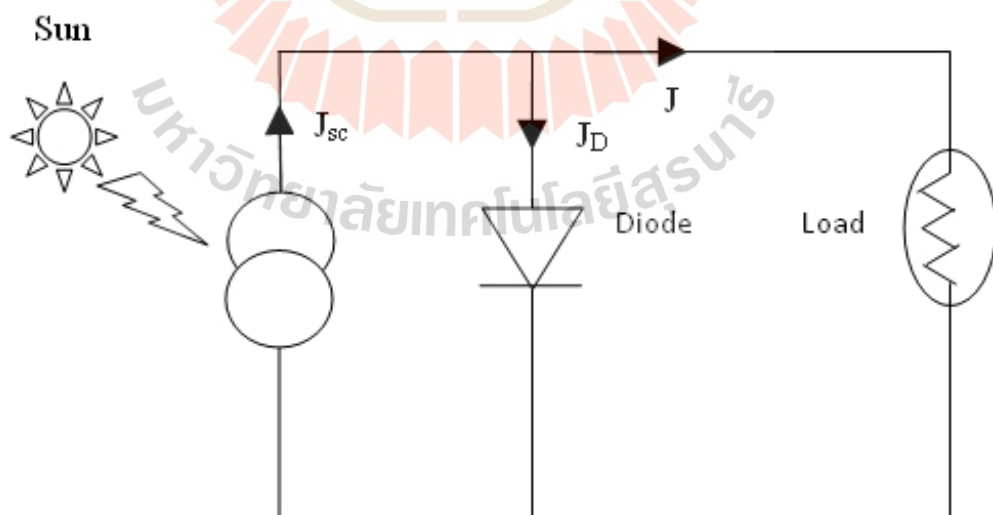


Figure 2.5 Solar cell equivalent circuits including diode inside.

Where: J_{sc} is current density from solar incident generating.

J is current density through external device.

J_d is current density through diode.

$$\text{While: } J_d = J_0(e^{(qV/KT)} - 1) \quad (2.4)$$

$$\text{And: } J = J_{sc} - J_0(e^{(qV/KT)} - 1) \quad (2.5)$$

So, in J versus V plot there is a point that gains the maximum power density (P_{max}) as shown in figure 2.6. Fill factor is the ratio between P_{max} and P_{total} and the solar cell efficiency (η) has been calculated from (P_{max} / P_{input}) when P_{input} is solar power (1000 W/m^2).

$$\eta = \frac{P_{max}}{P_{in}} = \frac{FF * V_{oc} * J_{sc}}{P_{in}} \quad (2.6)$$

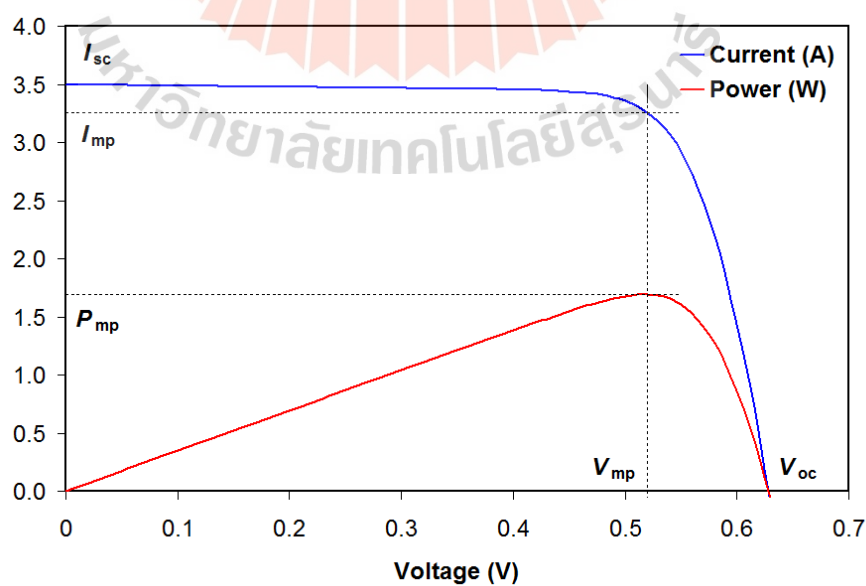


Figure 2.6 J-V curve of Solar cell (Squirmymcpee, Online, 2008).

However, every solar cell also has intrinsic resistant, including of series resistant (R_s) and shunt resistant (R_{sh}). Series resistant (R_s) is resistant between the electrode and solar cell that cause reducing the current and drop down the efficiency, shunt resistant (R_{sh}) is resistant between P and N junction and will block the current collector of electron and hold this will help to increase the efficiency of solar cells. The new equivalence circuit will change as a figure 2.7.

And new equation is as following:

$$J = J_s - J_0 \left(e^{q((V+J R_s)/KT)} - 1 \right) - \frac{V+J R_s}{R_{sh}} \quad (2.7)$$

The R_s and R_{sh} have effect of the characteristic of J-V curve as shown in figure 2.8 so in solar cell production, it needs to be increasing R_{sh} and reduce R_s .

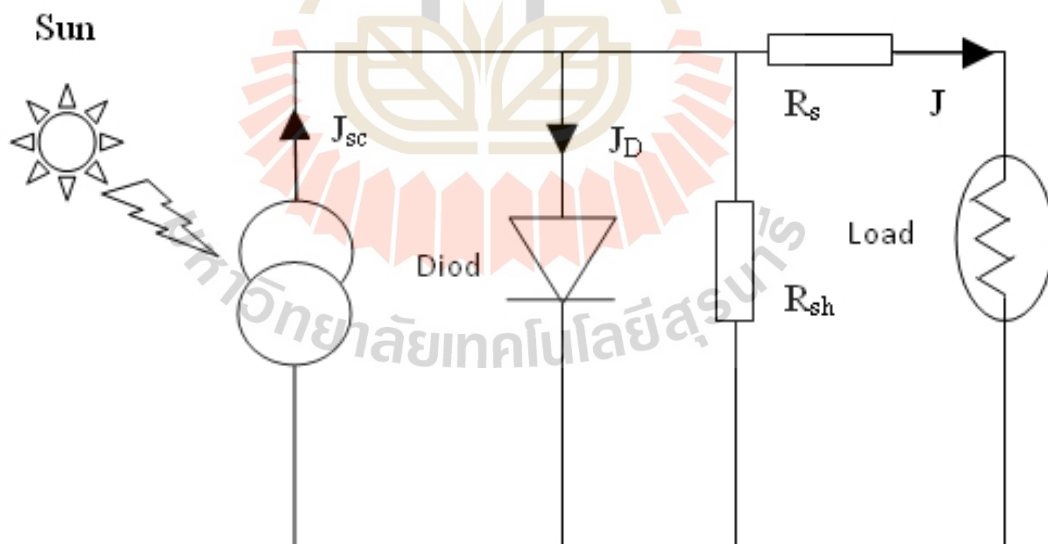


Figure 2.7 Solar cell equivalent circuits with including resistant.

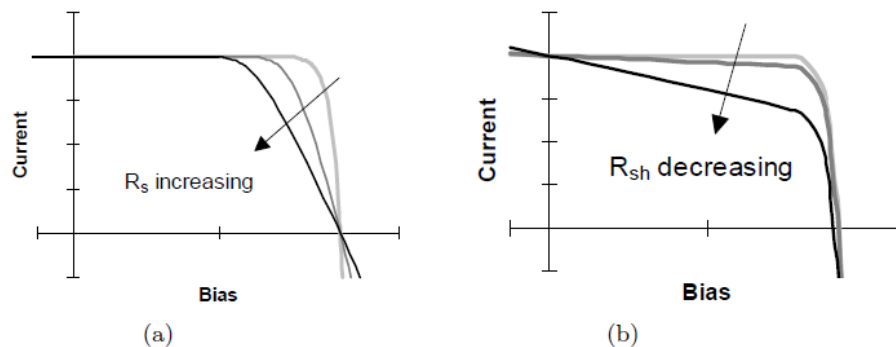


Figure 2.8 Effect of R_s and R_{sh} to J-V curve a) when R_s is increasing the area of curve was reduced and b) opposition of R_s when R_{sh} decreasing area of curve also decrease.

2.4 Dye-Sensitized Solar Cells

2.4.1 Structure

There are many different forms of DSSCs, the main structure is shown in the figure 2.9. This including of 1) conductive glass, using glass slide coated with metal oxide doped such as Indium doped Tin Oxide (ITO) or Fluorine doped Tin Oxide (FTO), 2) metal oxide layer (scaffold layer) using wide bandgap materials for transfer electron from dye-sensitizer to conductive glass and also use as host for dye adhesive, the metal oxide materials are TiO_2 which suitable for synthesis dye and ZnO which appropriate for natural dye, 3) the most important part is dye-sensitizer that must absorb photon energy and release electron, natural dye were attracted from leaf or other parts of tree and flower, however, the effect of natural dye is very low when compared with syntheses dye, 4) electrolyte or hole transporting layer, this part will take electron from counter electrode and give it to dye-sensitizer, 5) counter electrode, must be a catalyst for redox reaction of electrolyte and has a corrosion resistant of electrolyte.

2.4.2 Materials

Substrate

Because of light must pass through the substrate to absorbed by the sensitizer, a substrate must clear and transparent. Glass or plastic is the best choice for the substrate, glass is rigid and strong, but plastic is flexible. The electron transporting via substrate so it necessary to make substrate conductive. Transparent conductive films (TCFs) on the substrate can make from both inorganic and organic materials.

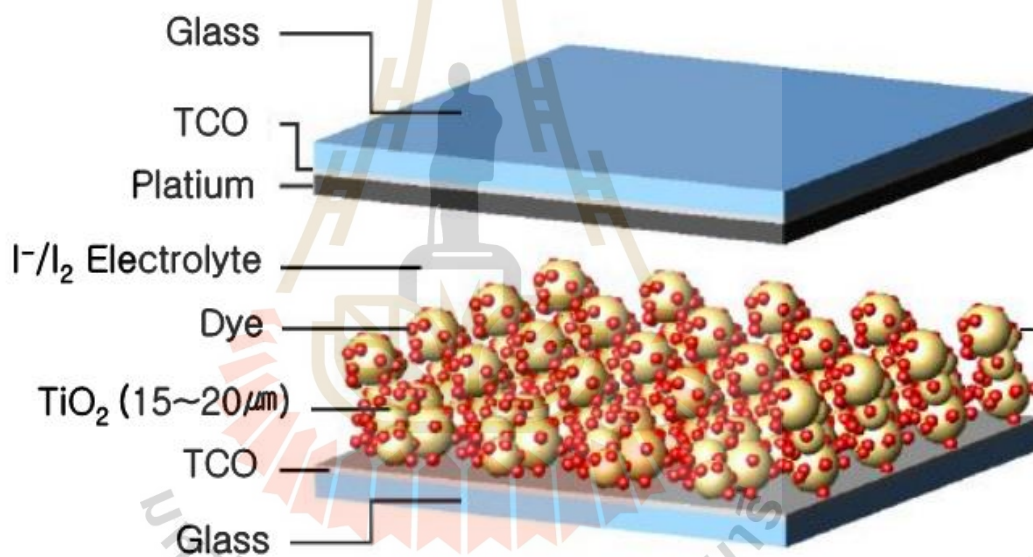


Figure 2.9 Structure of dye-sensitized solar cells (Fraunhofer Institut Solare Energiesysteme, 2011).

Inorganic films are made from oxides compounds such as indium tin oxide (ITO), fluorine-doped tin oxide (FTO) or doped zinc oxide, inorganic films are strong with high temperature so it appropriate for DSSCs production. Organic films are made by carbon nanotube or graphene materials with can make very high conductive films or

make from a conductive polymer with easy to make in the wide area. Organic films are flexible but so weak for a high-temperature process.

Scaffold layer

Scaffold layer or metal oxide layer is the host for dye attracting and take an excited electron from dye to give to a substrate. A band gap of this layer must be a wide range to cover energy level of dye-sensitizer. Titanium dioxide (TiO₂) is a typical use for inorganic dye because it has a wide band gap (3.2 eV), not expensive, transparent, and high melting point (2116 K). Zinc oxide (ZnO) also used in DSSCs for organic dye because of wide band gap (3.3 eV) and high electron mobility.

Dye sensitizer

Dye sensitizer is photosensitive materials which can absorb a photon and be generating electron. There are many types of dye sensitizer, a natural dye was extracted from plain and very cheap, but its effect is quite low (2%). Typically, dye sensitizer is synthesis from ruthenium complex material as core molecule and adjustable absorption by change a branch ring e.g. [Ru(4, 4' - dicarboxy - 2, 2' - bipyridine)₂(NCS)₂] or N3 dye, [Ru(4,4'4" - (COOH)₃ - terpy)(NCS)₃] or black dye and (cis - Ru(H₂dc bpy)(dnbpy)(NCS)₂ or Z907 dye. However, the most favorite dye for high efficiency and high stability is N719 (Di - tetrabutylammoniumcis - bis(isothiocyanato)bis(2, 2 - bipyridyl - 4, 4 - dicarboxylato)ruthenium(II)), structure of Ru dye is shown in figure 2.10.

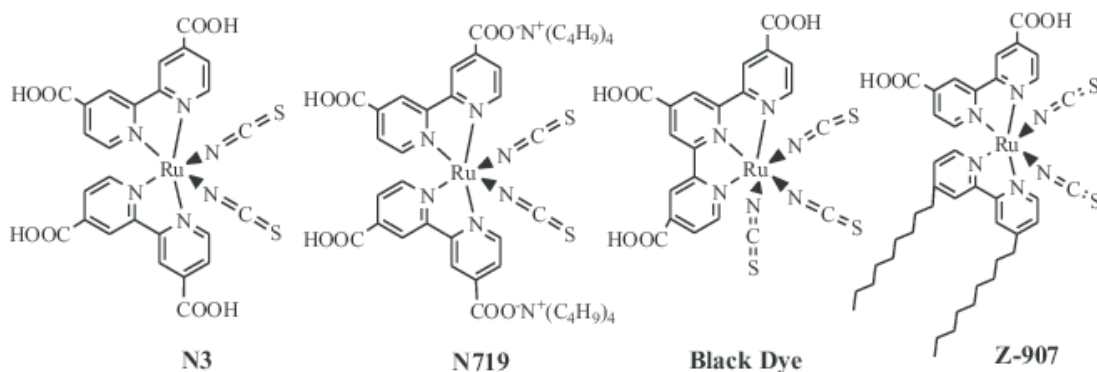


Figure 2.10 Structure of N3, N719, black dye and Z-907 sensitizers. (Giribabu, 2012).

Electrolyte

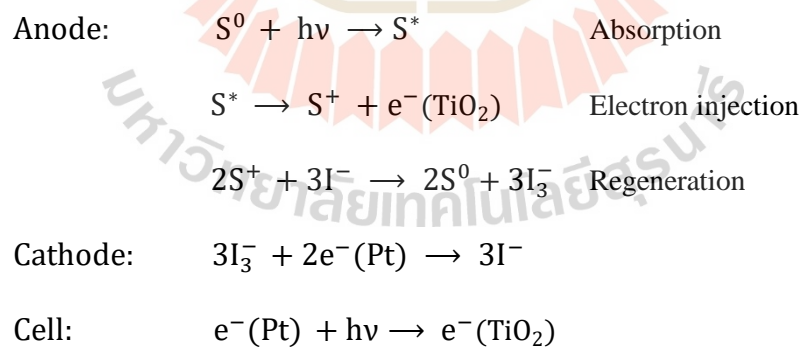
The electrolyte is responsible for transporting electron from the counter electrode to dye sensitizer molecule. For DSSCs almost electrolyte is liquid form and electron transport via redox reaction of the electrolyte. Redox reaction of complex iodine is most efficient and very high stability, by a couple state of 3I^- and I^{3-} can generate efficiency about 13%. Another system and new is a couple of Co^{2+} and Co^{3+} in cobalt electrolyte reaction, cobalt electrolyte is more environmentally friendly than iodine electrolyte.

Counter electrode

To collect electron and give it back to the cell, counter electrode must be a catalyst of electrolyte system and the work function of counter electrode should near with HOMO state of an electrolyte. Platinum is the best counter electrode for iodine electrolyte, it gives a highly efficient and well resistant to iodine corrosion. However, platinum is very expensive material, alternatives electrode such as carbon or conductive polymer is an aspect of replacing the platinum electrode.

2.4.3 DSSCs working principle

Dye-sensitized solar cells (DSSCs) is quite different from conventional solar cells (Si solar cells or thin films solar cells) because it not exactly based on a P-N junction. The photoelectron was generated from dye molecule then inject to the working electrode and after electron was used from external load it will come back to cell via counter electrode by following these step: 1) The electron in dye molecule absorbs the photon and go to excited state, this electron was called Exciton. 2) Exciton transport to the conduction band of metal oxide materials. 3) The electron injected from metal oxide layer to transparent conductive electrode. 4) The electron was used by an external device and come back to the cell at the counter electrode. The counter electrode will give the electron to cells by a redox reaction of electrolytes. 5) Electrolyte gives electron to HOMO state of dye-sensitizer to continue new circle. The chemical reaction and equation were written as:



The schematic diagrams of dye-sensitized solar cells (DSSCs) and electron transfer is shown in figure 2.11.

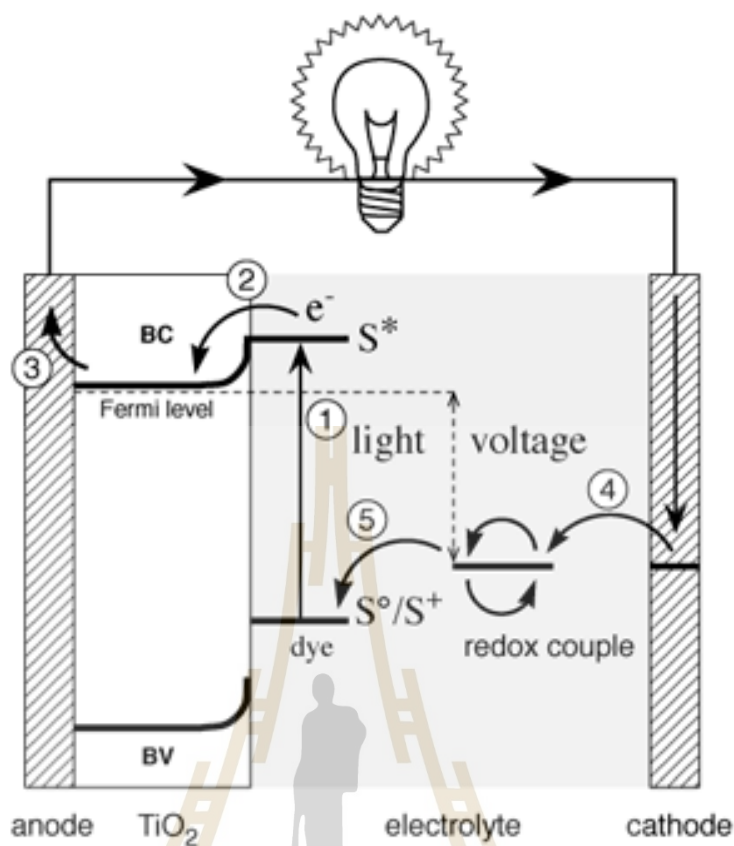


Figure 2.11 The schematic diagrams of dye-sensitized solar cells (DSSCs) (Solaronix, Online, 2008).

2.5 History of Diamondoids

In this thesis, the counter electrode of dye-sensitized solar cells was made by using diamondoids (nano size of diamond) as a precursor. The smallest molecule (single cage) is called adamantane and the bigger, tetramantane (4 cages) is also used for better efficiency. Diamondoids is perfect and complete SP^3 hybridization of carbon, the dangling bonds are bonding with hydrogen atoms as shown in figure 2.12. The smallest molecule of diamondoids (adamantane) was first discovered in 1933 in petroleum process (Landa et al., 1933) then its successful synthesis in 1941 by V. Prelog and R.

Seiwerth (Prelog and Seiwerth, 1941). The simple synthesis was developed in 1957 by Paul von Ragu Schleyer and became widely available (Schleyer, 1957). In 1965 Schleyer and Cupas successful in synthesizing a bigger molecule of diamondoids, Diamantane (Cupas et al., 1965) then one year after that 3-cage molecule, triamantane was synthesized (van Zandt et al., 1966). A higher structure seems difficult to synthesis, however, nowadays the highest synthesized diamondoids are three isomers of tetramantane (4 cage structure) (McKervey, 1980). On the other hand, extracting from petroleum still, develop. In 1966 diamantane was isolated (Hala and Landa, 1966). Onwards, many researching groups reported the discovery of diamondoids series from triamantane to hexamantane (Wingert, 1992) during the 1990s and the sized up to 11 crystal cages in 2003 by Jeremy Dahl (Dahl et al., 2003). The picture of diamondoids crystal is shown in figure 2.13.

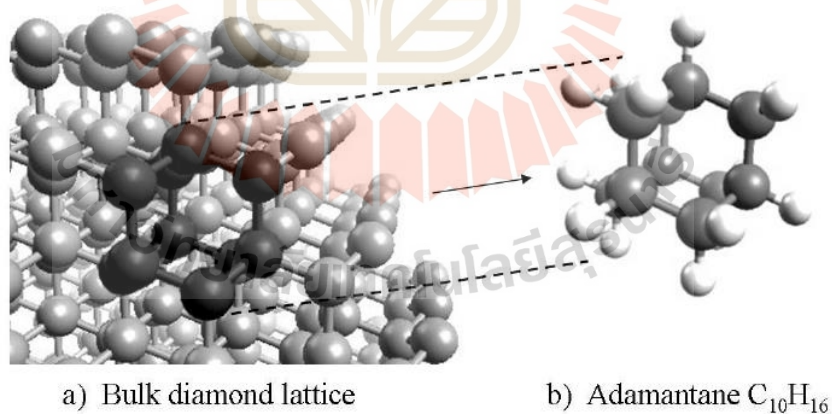


Figure 2.12 Adamantane (C₁₀H₁₆) is the smallest closed-cage diamond nanostructure. In a top-down approach it can be constructed by excising a single crystal cell from the bulk diamond lattice (a) and then passivating dangling bonds with hydrogen (b). (Lasse Landt, 2010).



Figure 2.13 Different diamondoids recrystallized in macroscopic amounts as vander-Waals crystals (Lenzke et al., 2006).

2.6 Electronics Properties of Diamondoids

To make a better DSSCs from diamondoids, the electronics properties of diamondoids must clearly understand. Starting with the energy levels state, using the X-ray absorption spectra (XAS) to investigate the lowest unoccupied molecular orbitals (LUMO) and X-ray photoemission spectroscopy (XPS) to investigate the highest occupied molecular orbitals (HOMO). The X-ray absorption spectra of carbon K-edge as shown in figure 2.14 indicated LUMO state is fixed and independent of the size of diamondoids. This character is a contrast to similar materials, such as Si or Ge-

nanocrystal which the conduction state will shift according to size increasing (van Buuren et al., 1998; Bostedt et al., 2004).

Whereas the X-ray photoemission spectroscopy information indicated HOMO state of diamondoids is depended on a size of the molecule as shown in figure 2.15. The HOMO energy shifting to lower binding energy when the size of diamondoids is increasing, where the LUMO was fixed meaning the bandgap of diamondoids was decreased with size-increasing as shown in table 2.1.

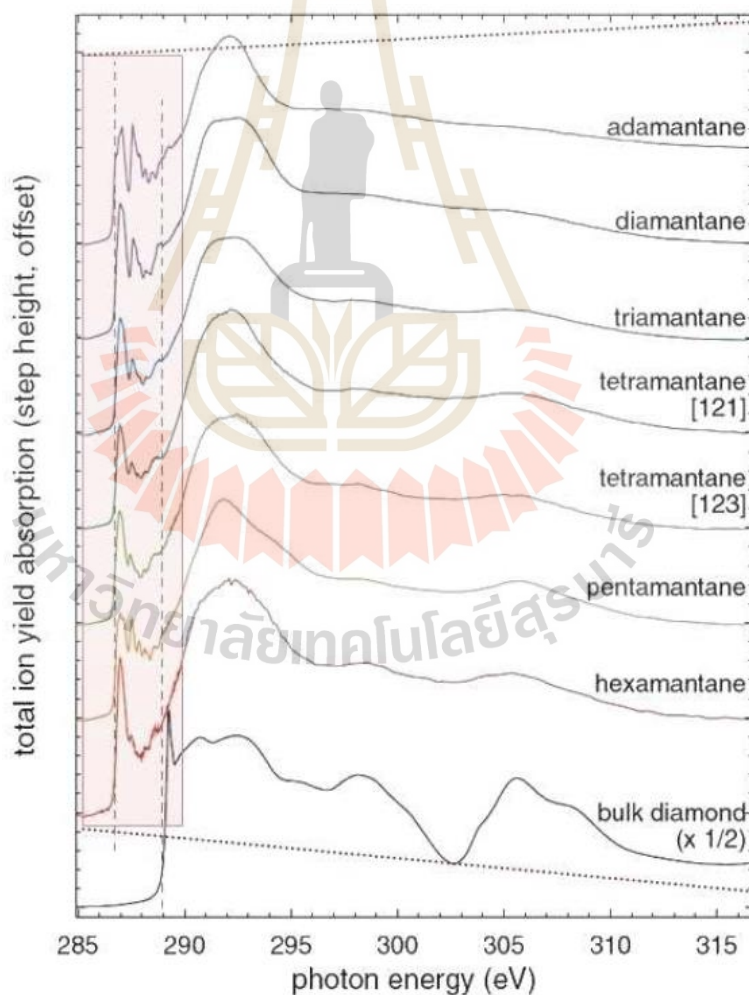


Figure 2.14 X-ray absorption spectra of pristine diamondoids (Willey et al., 2005).

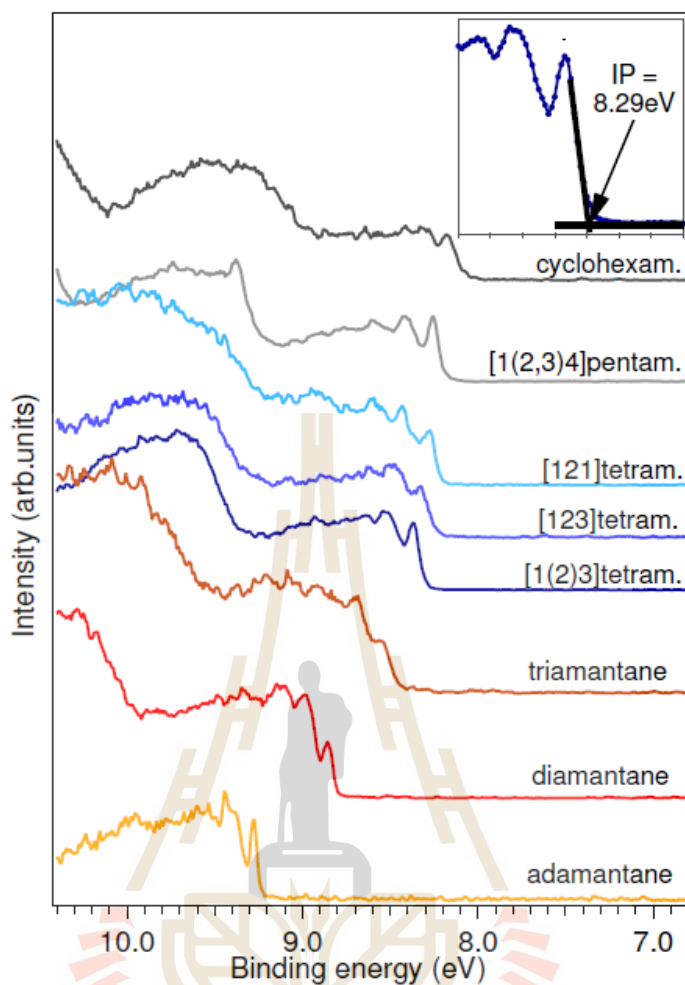


Figure 2.15 Valence band photoelectron spectra for a series of diamondoids. The inset shows the determination of the ionization potential (IP) by the interpolation method using the example of [1(2)3] tetramantane (Landt et al., in preparation).

Moreover, the low kinetic energy region from photoelectron spectroscopy (PES) of diamondoids shown very high and sharp peak, different from other materials. In 2007 Yang and co-worker (Yang et al., 2007) was observed this characteristic and explained that diamondoids exhibit negative electron affinity, with the vacuum level is below than conduction band, when electron was excited to conduction band it will go

to vacuum level instead of returning to valence band, and meaning diamondoids can be emitted electron itself. The schematic diagram is shown in figure 2.16.

Table 2.1 The first ionization potentials as measured by photoelectron spectroscopy (PES) (Landt et al., in preparation).

Diamondoids name	PES (eV)
adamantane	9.23
diamantane	8.80
triamantane	8.44
[121] tetramantane	8.20
[123] tetramantane	8.22
[1(2)3] tetramantane	8.29
[1(2; 3)4] pentamantane	8.18
[1234] hexamantane	8.00

In 2015, Narasimha and co-worker (Narasimha et al., 2015) discovered diamondoids monolayer can reduce the surface work function of gold substrate and very stable as shown in figure 2.17. The largest work function reduction was found in 6TT (3.38 eV) and 2TT (3.50eV) of a tetramantane-thiol molecule (-thiol is a functional of sulfur on dangling bond of carbon). The lowest work function after reducing is 1.60 eV for 2TT and 1.72 eV for 6TT, these are equivalent to the lowest work function with observed from inorganic Cs-coated Au (1.6eV) (LaRue et al., 2008). This behavior of diamondoids should help counter electrode easy to return electron to DSSCs.

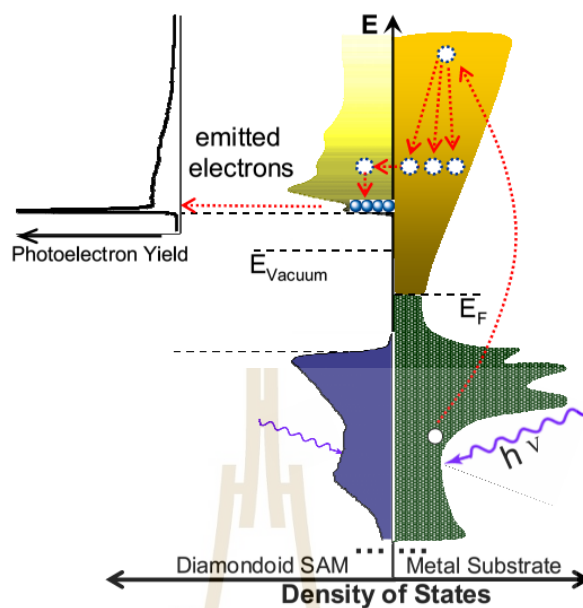


Figure 2.16 Schematic diagram of the electron-emission process on diamondoid SAM surfaces. E_F is the Fermi level of the metal substrate, sitting in the energy gap of diamondoid. The vacuum level (E_{vacuum}) is below the conduction-band minimum of the diamondoid, a characteristic of NEA (Yang et al., 2007).

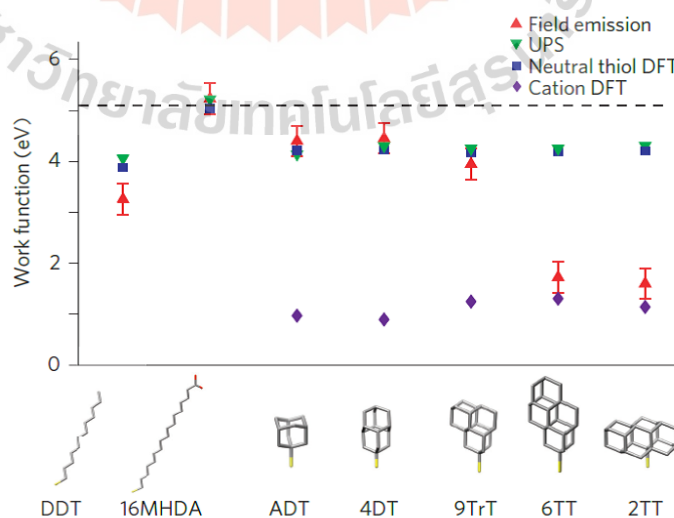


Figure 2.17 The reducing of work function from diamondoids (Narasimha et al., 2015).

2.7 Summary

This section shows the information of the history of solar cells, three generation of solar cells, the working principle of solar cells with including of the spectrum from the Sun on the Earth ground and solar cell circuit. For dye-sensitized solar cells parts, consist of the structure of DSSCs, materials of each part of DSSCs and DSSCs working principle. Finally, is information of diamondoids with was chooses as the main precursor of this thesis, including of history and electronic properties of diamondoids.



CHAPTER III

CONSTRUCTION AND TESTING OF DYE-SENSITIZED SOLAR CELLS

This section was set to describe DSSCs fabrication, cells construction, method, and device selection for testing and characterizing materials. Dye-sensitized solar cells (DSSCs) consist of three parts, a working electrode, electrolyte, and counter electrode. Each part preparation was explained in this section.

3.1 Material and Instrument Selection

3.1.1 Material Selection

Materials were used in this thesis are as followings. Firstly adamantane (99%, $C_{10}H_{16}$, Molecular Weight 136.23, Aldrich company) were used as precursor of CVD technique. 1-adamantanethiol (95%, $C_{10}H_{16}S$, Molecular Weight 168.30, Aldrich company) and [121]tetramantane-6-thiol ($C_{22}H_{27}S$, Wanli Yang, ALS.) were used for self-assembled monolayer (SAMs) technique. FTO glass (F – SnO_2 coated glass, sheet resistance of 8 ohms/sq., Solaronix Company) was used as working electrode substrate. Tungsten boat source (Kurt J. Lesker company) and N-type Si were used as substrate of CVD technique. TiO_2 PST-18NR (CATALYSTS & CHEMICALS IND Company)

transparent paste were used as scaffold layer. TiO₂ PST-400C (CATALYSTS & CHEMICALS IND Company) paste were used as scattering layer. N719 (cis-Bis(2,2'-bipyridyl-4,4'-dicarboxylato) diisothiocyanatoruthenium (II) Ditetrabutylammonium, Solaronix Company) and Y123 were used as sensitizer. Ethyl alcohol, Isopropanol, tert-butanol, and acetone nitrile were used to dissolve dye-sensitizer and electrolyte. 1-Methyl-3-propylimidazolium iodide (MPI- (C₇H₁₃N₂I) , 99%, Fluka Company), Lithium iodide anhydrous (LiI, 98%., Fluka Company), Iodide (I₂, 99.5%, Riedel-dehaen Company), Tert-Butylpyridine (TBP, 98%, Fluka Company) and Lithium carbonate (LiCO₃, 99.99%, Aldrich Company) were used to prepare electrolyte.

3.1.2 Testing Techniques

The purpose of this thesis is to make solar cell device, howsoever films characterizing is a need for understanding intrinsic properties. Including of Conductive Atomic Force Microscopy (C-AFM) for study topology of films and measuring localize resistant, Impedance Analyzer for study overall resistant, Cyclic Voltammetry for study redox reaction between electrolyte and counter electrode, Photoemission Spectroscopy (PES) for investigating electronic structure and energy alignment of films and Solar Simulator for measuring solar cell efficiency.

Solar Simulator

A solar simulator is the main testing instrument for measuring the solar cell efficiency. The solar simulator is the device for simulating the indoor sunlight and controllable intensity. The solar simulator is also used for testing other application such as photolysis of water, sunscreen protecting performance and dye degradation. Quality

or class of solar simulator was classified by three factors including of spectral content, spatial uniformity, and temporal stability. The standard criterion of solar simulator was set according to the IEC 60904-9 Edition2 and ASTM E927-10 standards (Specification for Solar Simulation for Photovoltaic Testing. 2010. doi:10.1520/E0927-10). There are three classes, A, B or C class upon to data in the table 3.1.

Table 3.1 ASTM class specifications.

Classification	Spectral Match	Spatial Non-Uniformity	Temporal Instability
Class A	0.75 - 1.25	2%	2%
Class B	0.60 - 1.40	5%	5%
Class C	0.40 - 2.00	10%	10%

Generally, the solar simulator was made from xenon arc lamp with provide a continuous spectrum and most matching to sunlight spectrum. However, xenon arc lamp has some sharp peak at 800nm to 900nm wavelength with different from sunlight and filter is needed to solve this problem. After filtering the spectrum from solar simulator should be more like sunlight in each wavelength intervals as shown in table 3.2. A new type of solar simulator lamp with can control the intensity of each wavelength is light-emitting diodes (LED) but the intensity is not high as from xenon arc lamp and still expensive. This thesis choosing Solar simulator, PEC-L11 (Japan) with classified in AAA standard spectrum.

Table 3.2 ASTM spectral irradiance for three standard spectra.

Wavelength [nm]	AM1.5D	AM1.5G	AM0
300-400	no spec	no spec	8.0%
400-500	16.9%	18.4%	16.4%
500-600	19.7%	19.9%	16.3%
600-700	18.5%	18.4%	13.9%
700-800	15.2%	14.9%	11.2%
800-900	12.9%	12.5%	9.0%
900-1100	16.8%	15.9%	13.1%
1100-1400	no spec	no spec	12.2%

Impedance Analyzer

Impedance analyzer or Electrical Impedance Spectroscopy (EIS) is an instrument for measuring the alternating current when an alternating voltage is applied. This technique can observe the resistance and phase of impedance in both real part and imaginary part then we can plot data in the complex impedance plan as shown in figure 3.1.

From figure 3.1, in cartesian form, impedance is defined as:

$$Z = R + jX \quad (3.1)$$

Where R is a real part of impedance refer to resistant of materials and X is imaginary part of impedance depend on responding of capacitance (C) and inductance

(L) to the applying voltage frequency. While $Z_R = R$ is ideal resistor independence of applying voltage frequency, R is dominating in only real part. $Z_L = j\omega L$ and $Z_C = 1/(j\omega C)$ where ω is angular frequency and dominating in imaginary part. So, impedance Z is depending on angular frequency, by varying of angular frequency the impedance plotting will change in impedance plan and the character of impedance can give information of resistant, capacitance and inductance of materials. The impedance of DSSCs can measure in two modes: symmetrical of the counter electrode and complete cells as shown in Figure 3.2. After fitting model parameter, the value of series resistance (R_s), charge resistance (R_{ct}) and capacitance will be extracted. In this thesis, choosing FRA32M - Impedance analysis, Metrohm Autolab for wide frequency range (0.01 Hz to 200kHz) analysis.

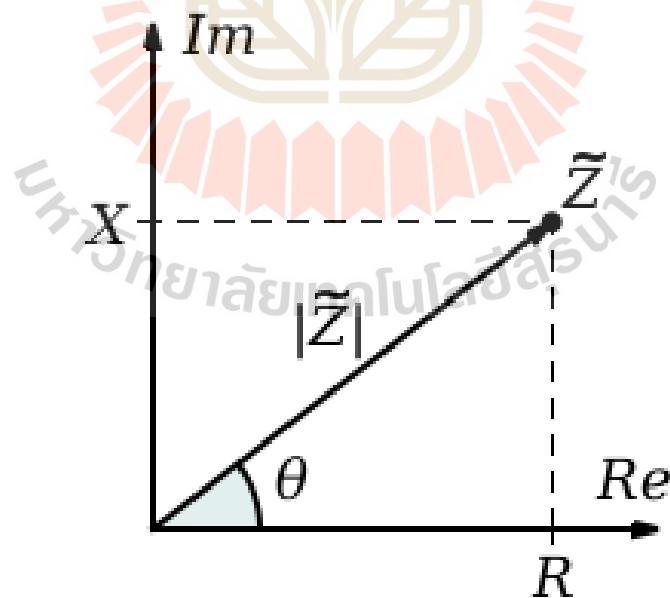


Figure 3.1 A graphical representation of the complex impedance plane.

Cyclic Voltammetry

Cyclic voltammetry (CV) is used to measure the current between electrode after applying ramps linearly potential versus time in cyclical phases as shown in Figure 3.3. The experiment method is set in three electrodes by our DSSCs counter electrode is installing in the working electrode of CV system, a counter electrode of CV system is platinum wire and using Ag/AgCl as referent electrode. The potential was applied and measured between the working electrode and referent electrode while the current is measuring between the working electrode and counter electrode of CV system. The result from CV measurement should be leaf-like as see in a figure 3.4. The current-potential curve shows a redox reaction of electrolyte and the working electrode, a forward peak present oxidation reaction of electrolyte and backward investigating reduction of the electrolyte. The CV can use to comparing redox reaction rate between the electrode to select the best electrode for DSSCs.

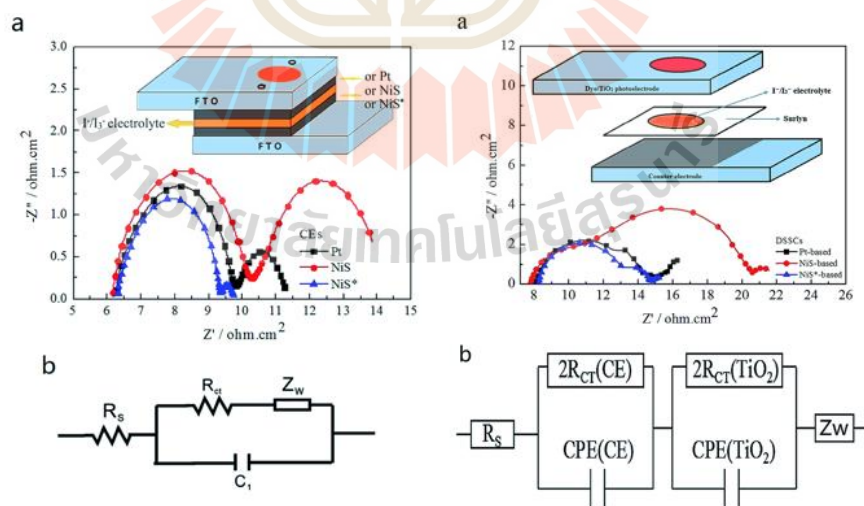


Figure 3.2 Impedance model of DSSCs a) symmetrical setup with c) the impedance model of symmetrical cell and b) real cell setup with d) the impedance model of real cell (Yue et al., 2014).

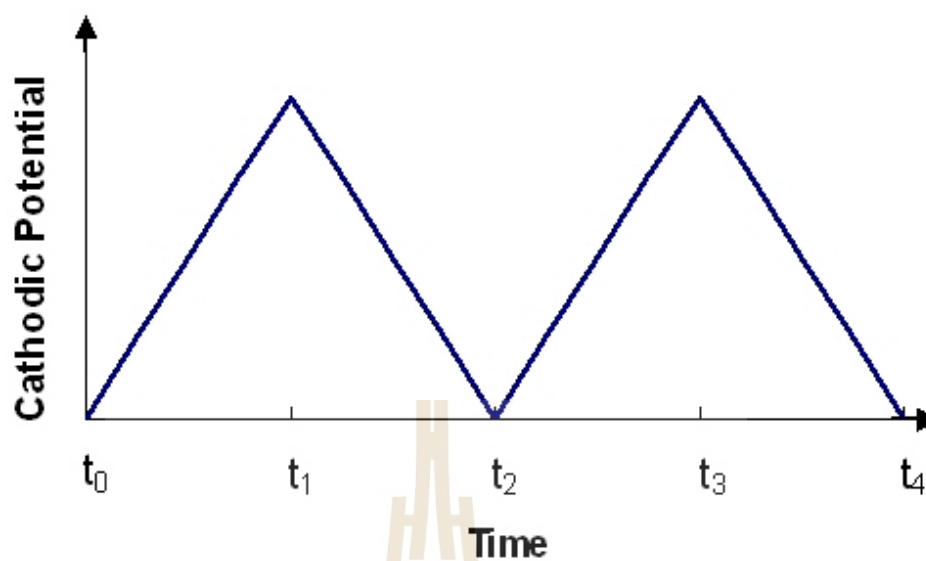


Figure 3.3 Cyclic voltammetry waveform (Timothy, Online, 2006).

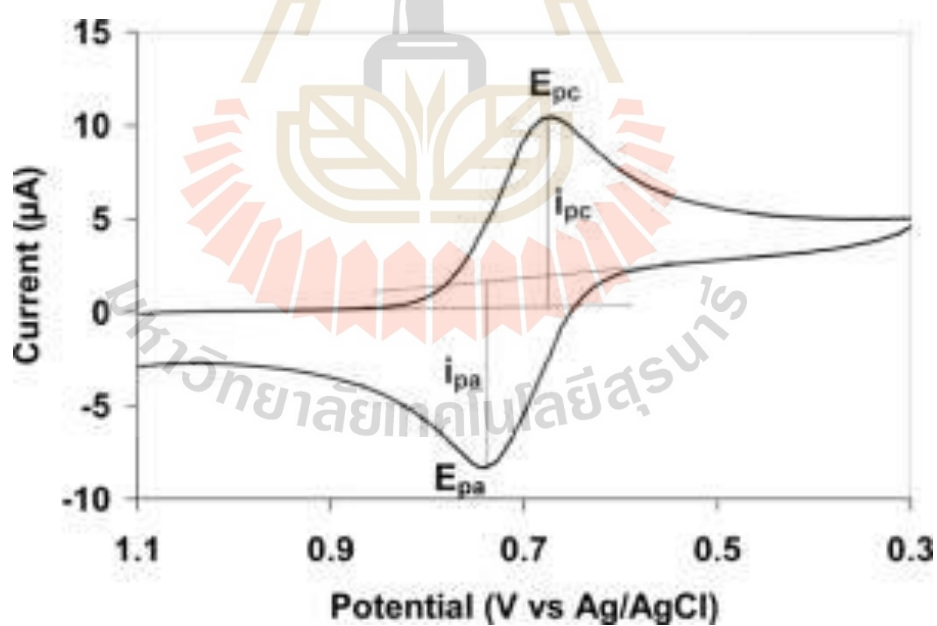


Figure 3.4 Typical cyclic voltammogram where and show the peak cathodic and anodic current respectively for a reversible reaction. The y-axis shows the negative current (Lifer21, Online, 2005).

Photoemission Spectroscopy

X-ray photoemission spectroscopy (XPS) is a technique using the photoelectric effect theory to be analyzing the surface properties of a material. By irradiating a solid surface with X-ray (or UV beam) and measuring the kinetic energy and amount of electrons that are emitted from the surface of the material, we can obtain the elemental composition, chemical binding energy and electronic state of elements as shown in figure 3.5. Binding energy (BE) represents the energy that must be done against the force which holds an electron and nucleus together. Each atom in the surface has core electron with the characteristic of binding energy and equal to ionization energy of an electron. The binding energy of the electron is given by the Einstein relationship.

$$BE = PE - E_k - W \quad (3.2)$$

where: PE is incident photon energy, E_k is kinetic energy of electron, and W is work function of material.

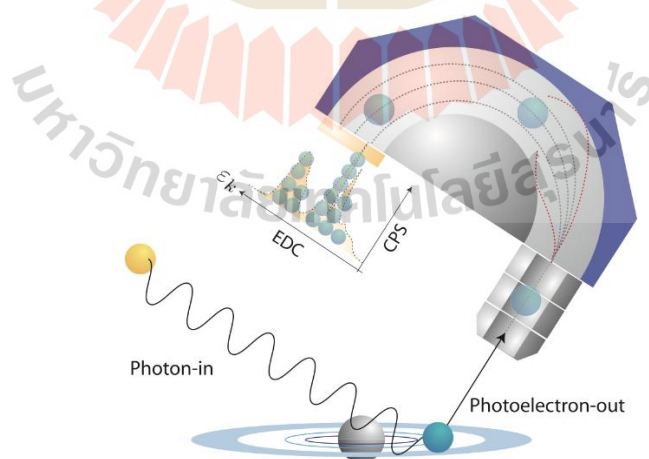


Figure 3.5 XPS system (SLRI, Online, 2016).

Conductive Atomic Force Spectroscopy

Conductive Atomic Force Microscopy (C-AFM) is a mode of atomic force microscopy using a conductive tip in contact mode to scan the sample surface. The voltage is applied between the tip and the sample during a scan to measure a current image. At the same time, a topographic image is also measured from the same point (see figure 3.6). In this thesis, we use Park XE-100 AFM (Park system) located at the F-10 building, Suranaree University of Technology (SUT).

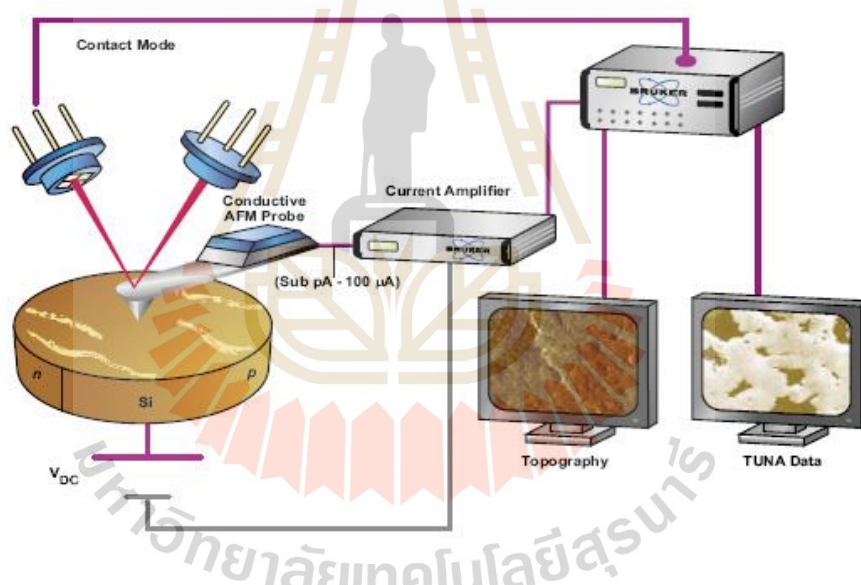


Figure 3.6 Conductive Atomic Force Microscopy (Brukerafmprobes, Online, 2017).

3.2 Working Electrode Preparation

3.2.1 Substrate Cleaning

For working electrode, fluoride doped tin oxide (FTO glass, a sheet resistance of $8\Omega=\text{sq}$, Solaronix) was chosen for high-temperature annealing process. This start

with cutting FTO glass to 1.5 cm x 2.0 cm and cleaning by take it in an ultrasonic bath with a detergent solution for 10 mins and washed by deionized water then following by taking ultrasonic in acetone solution 10 mins and in ethanol 10mins finally is washed by deionized water again and drying by a hair dryer.

3.2.2 Blocking Layer Deposition

After cleaning, a first layer was deposited on the substrate. This thesis is choosing compact TiO_2 as a hole blocking layer to prevent electron recombine to hole because compact TiO_2 is transparent and an energy level is like TiO_2 scaffold layer. FTO was covered by PI tape to make a pattern then put into a beaker, the TiCl_4 solution is mixing of TiCl_4 and deionized water 1:10 v/v was poured into the beaker. After heating to 80 °C for 30 mins compact TiO_2 were forming on the surface of FTO glass then films were drying on the hotplate at 80 °C for 10 mins.

3.2.3 TiO_2 Scaffold Layer Coating

TiO_2 scaffold layer was coating on blocking layer by screen printing technique, the mask of the screen is 90T (90 line/inch), and active area is 0.25 cm x 1.0 cm. TiO_2 (PST-18NR), the mesoporous molecule of TiO_2 mixed with binder polymer was screen printing by manual then dry in the air for 10 mins and heated on the hotplate at 80 °C for 10 mins. After films cooled next layer was repeated until 5 layers of TiO_2 was deposited. To improve the efficiency, TiO_2 scattering (PST-400, a bigger molecule of TiO_2) was deposited by the same technique for reflecting remain photon. This film was

finally annealing at 500 °C for removing the dissolving polymer. The thickness of TiO₂ was investigated by scanning electron microscope (SEM) and found as 50 μm.

3.2.4 Dye-Sensitizer Coating

Before immersing in the dye solution, working electrode films were treated by UV-ozone for 10 mins to cleaning the surface and make the better hydrophilic attraction. Dye-sensitizer solution is mixing of 0.3 mM of N719 [(cis-bis (isothiocyanato) bis (2,2-bipyridyl4,4dicarboxy-lato) – ruthenium (II) - bistetrabutylammonium)] in acetonitrile/tert-butanol 1:1, v/v. After films immersed in the dye solution for 24 hrs, films were rinsed by ethanol for removing non-contact dye and drying in air for fabricating in next step.

3.3 Counter Electrode Preparation

3.3.1 Sputter deposition

Sputtering technique is physical vapor deposition (PVD). The films were ejected from target materials by Collider of an inert gas atom (e.g. Ar gas). There are many types of sputtering technique such as DC-sputtering, magnetron sputtering and RF-sputtering. A free electron was accelerated and collide Ar gas, Ar atom will be Ar⁺ and will be accelerated to collide the target as shown in figure 3.7. For DC-sputtering target must be conductive or metal materials, RF-sputtering target can be an insulator. The sputtering technique was chosen for depositing thin films for various application such as coating for protecting surface for preventing oxidation or coating conductive materials for better electrical contact. In this thesis will use this technique for depositing

platinum and gold materials on the substrate to make a referent counter electrode and for SAMs technique. The sputtering coater in this thesis is Mini Plasma Sputtering Coater GSL-1100X-SPC12-LD from MTI Corporation, USA.

3.3.2 Chemical Vapor Deposition (CVD)

Chemical vapor deposition (CVD) is a chemical process for depositing thin films of various materials. By using vapor of precursor which react and decompose on the substrate surface (see figure 3.8). For CVD of carbon normally they use methane gas or hydrocarbon vapor as a precursor. The setup of CVD systems includes furnace system with quartz tube connected to pump and gauge pressure and the other side of tube connects to the evaporating system. Evaporation system consists of evaporation tube with the view port and valve connecting to the quartz tube and inert gas line plate on the heater as shown in figure 3.9. In this thesis, CVD system was setup and installing by buying parts from MTI Corporation, USA.

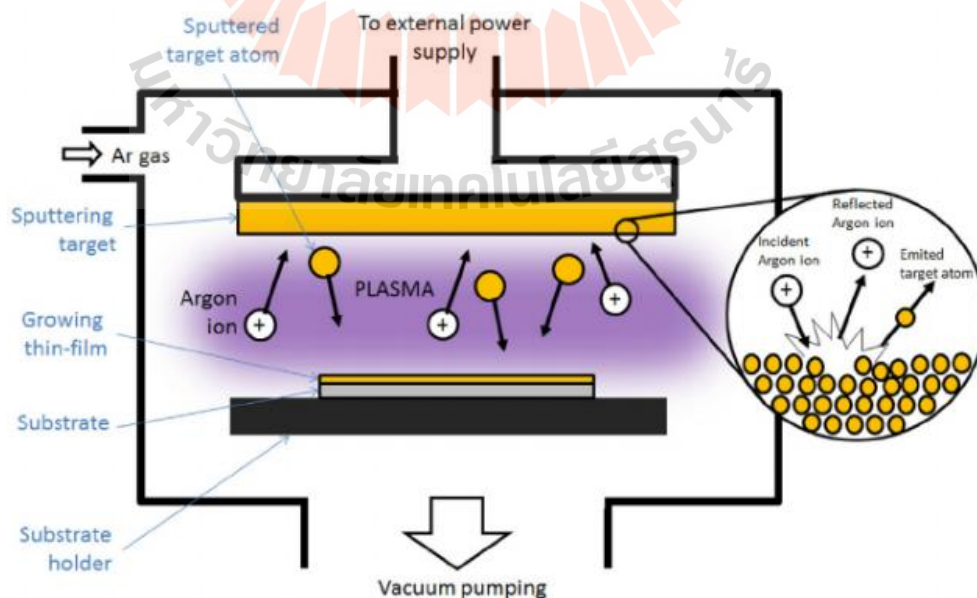


Figure 3.7 Schematics of the sputtering process (Pessoa et al., 2014).

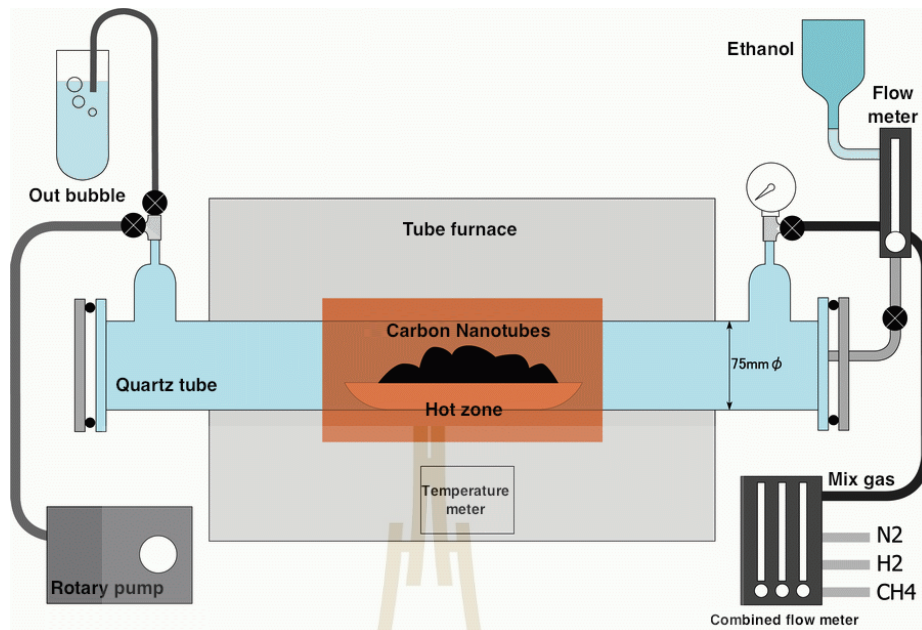


Figure 3.8 Chemical vapor deposition (CVD) system (NaBond Technologies Co., 2017).

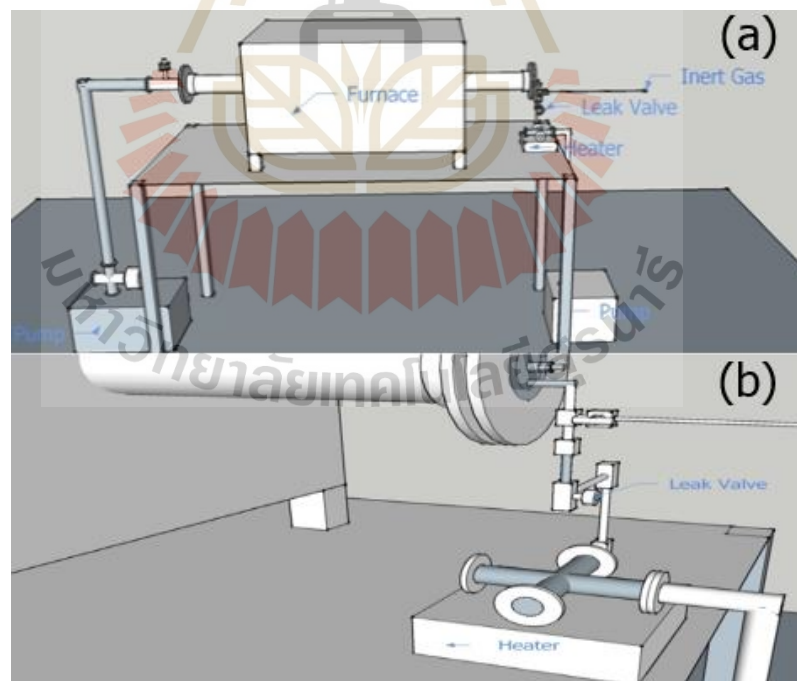


Figure 3.9 a) The experimental setup of furnace system. b) Evaporation system.

3.3.3 Self Assembled Monolayer (SAMs)

Self-assembled monolayers (SAMs) technique or direct immerse is very easy, by immersing a gold substrate in diamondoid with thiol solution and leave it over the night diamondoids will self-assemble on the gold substrate. The diamondoids solution consisting of 100 mg of diamondoids-thiol (adamantane-thiol, [121]tetramantane-6-thiol) in ethanol/toluene 9:1, V/V. The deposit time depends on substrate and solution, 24 hrs. for adamantane-thiol on the gold substrate, 7 days for adamantane-thiol on a platinum substrate and 1 hr. for [121]tetramantane-6-thiol on the platinum substrate.

3.4 Electrolyte Preparation

As a scaffold layer is porous materials, the liquid electrolyte should better for DSSCs. However liquid electrolyte has a drawback with a low mobility of charge transfer. Up to date, there are two redox couple with appropriate for DSSCs as following.

3.4.1 Iodine Electrolyte Preparation

Iodine couple is the first system was used in DSSCs and have been developing to improve efficiency until now. Nowadays, Iodine electrolyte is preparing by the mixing of 0.05 M iodide (I_2), 0.10 M lithium iodide (LiI), 0.60 M of 1,2-dimethyl-3-propylimidazolium iodide, 0.025 M lithium carbonate (Li_2CO_3) and 0.50 M of 4-tert-butylpyridine (TBP) in acetonitrile as previously reported (Saekow et al., 2012).

3.4.2 Cobalt Electrolyte Preparation

The cobalt complex, $[\text{Co}(\text{bpy})_3](\text{PF}_6)_2/[\text{Co}(\text{bpy})_3](\text{PF}_6)_3$ were prepared according to the reported procedure (Kim et al., 2011). 1.0 g (4.12 mmol, excess) of $\text{CoCl}_2 \cdot 6\text{H}_2\text{O}$ and 2.2 g (13.94 mmol, excess) of 2,2-bipyridyl were dissolved in 100 ml of methanol and refluxed for 2 h. After the solution was cooled to room temperature, 3.4 g (20.86 mmol, excess) of NH_4PF_6 was added to the mixture. The precipitate was filtrated and dried to obtain $[\text{Co}(\text{bpy})_3](\text{PF}_6)_2$. For $[\text{Co}(\text{bpy})_3](\text{PF}_6)_3$ 500 mg (0.612 mmol) of $[\text{Co}(\text{bpy})_3](\text{PF}_6)_2$ was taken out and added 107 mg (0.916 mmol, excess) of NOBF_4 in 15 ml of acetonitrile to increase oxidation at room temperature for 30 minutes. After filtrated, the residue was dissolved in 5 ml of acetonitrile and added 502 mg (3.08 mmol, excess) of NH_4PF_6 was added to the solution. The precipitate was filtrated and dried to obtain $[\text{Co}(\text{bpy})_3](\text{PF}_6)_3$.

3.5 Dye-Sensitized Solar Cells Construction

To fabricate DSSCs, first is to clean conductive glass then coat metal oxide by screen printing in this thesis we use TiO_2 as metal oxide and anneal to remove the dissolving polymer then immerse in dye solution over night for counter electrode we prepare by CVD technique and also sputtering Pt on W for referent cell and sputtering Au on W for the direct immerse technique we use para film to separate the electrode then drop a bit of electrolyte before complete assembly and measure the efficiency as shown in figure 3.10.

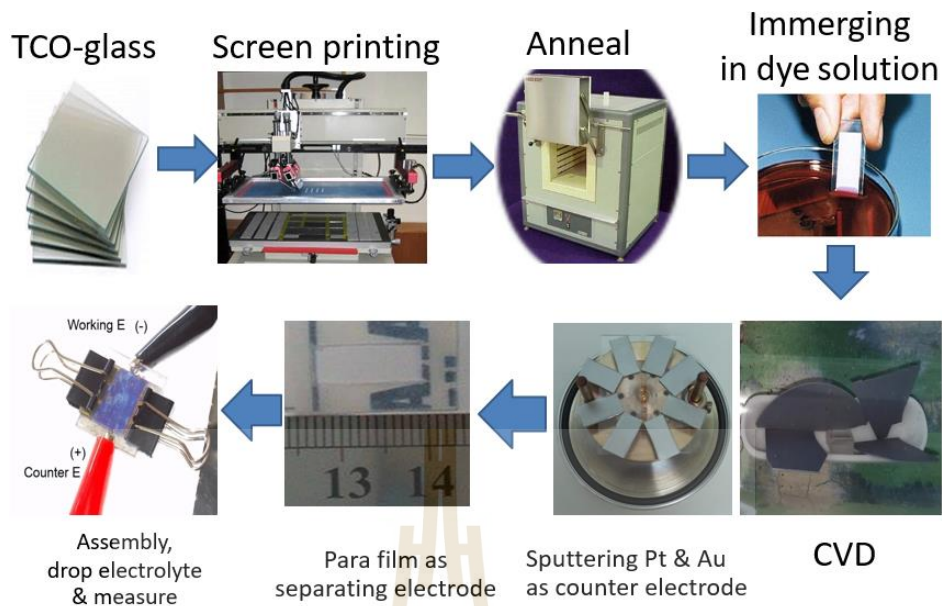


Figure 3.10 The DSSCs fabrication and processes.

3.6 Summary

The conclusion of this chapter are materials was choosing the lab grade product for the best result and there are many testing instruments for characterizing including of standard solar simulator, Electrical Impedance Spectroscopy (EIS), Cyclic voltammetry (CV), X-ray photoemission spectroscopy (XPS) and Conductive Atomic Force Microscopy (C-AFM). The dye-sensitized solar cells fabrication also detailing follow by Working Electrode Preparation, Counter Electrode Preparation, Electrolyte Preparation and Dye-Sensitized Solar Cells Construction. After many try until the best condition was found the next chapter will show an existing result of this thesis.

CHAPTER IV

RESULT ANALYSIS AND DISCUSSION

This chapter will show the result of thesis and analyses physical properties then discussion of the result. According to using tester equipment in the previous chapter, the result will explain in term of DSSCs efficiency, the effect of resistant from impedance result, the redox reaction from CV, electronic properties from PES then energy alignment will conclude the result.

4.1 Expected Result

The purpose of this thesis is to make a better counter electrode of dye-sensitized solar cells. Because of the novel material, Platinum is the best counter electrode in the term of highly efficient and good stabilize, even so, platinum is very expensive, the alternative counter electrode or developing from platinum is necessary. We choose diamondoids because of a strange in electric properties and expected it should help to improve efficiency and stability of DSSCs, another reason is self-assembled monolayers (SAMs) technique is very easy to process. This may reduce the cost per energy conversion of DSSCs and expect to bring DSSCs to use in worldwide.

4.2 J-V curve and Efficiencies

4.2.1 Iodine Electrolyte

As explained in Chapter II, the plotting between current density (J) and voltage (V) across solar cell electrode or J-V curve is the characteristic of solar cells. J-V curve give a lot of detail including of the efficiency, by defining the power density (P) is current density (J) multiply with voltage (V) then plotting P vs V there a maximum value of P, the ratio between P_{max} and P_{input} (P_{input} = 100 mW/cm²) is the efficiency of solar cell. J-V curve also shows the highest current density (J_{sc}) with relating to dye absorption and electron generation, the J-V line at a crossing of voltage axis is called open circuit voltage (V_{oc}) with relating to the energy in band alignment. Moreover, fill factor in J-V curve gives an information about the inside resistant of solar cells. After many testing, we found diamondoids can improve the efficiency of DSSCs, the best result of this research is the counter electrode which prepared via self-assembled monolayer technique by using the 4 cages structure [121]tetramantane-6-thiol as a precursor on the gold substrate (see figure 4.1). J-V curve shows a very high current density (J_{sc}) from diamondoids (27.50 mW/cm²) comparing to lower from platinum referent counter electrode (19.50 mW/cm²) and a little bit more of V_{oc}. The extreme current density leading the efficiency from [121]tetramantane-6-thiol up to 10.95% while from platinum is only 8.55%, this increasing about 28%. Not only from a big molecule of diamondoids, the 1 cage structure adamantane-thiol also give a good result by the short-circuit current density (J_{sc}) is 21.53 mW/cm² and the efficiency is 8.76%, higher than from Pt electrode as shown in Figure 4.2. The extreme large in current density and efficiency will be explaining in next section. Even though a very good effect, there is a critical drawback from diamondoids on the gold electrode. Because iodine electrolyte was destroying gold substrate, this makes the corrosion of

diamonoids films and the efficiency was quickly decrease and the cell was died in a few seconds as shown in figure 4.3.

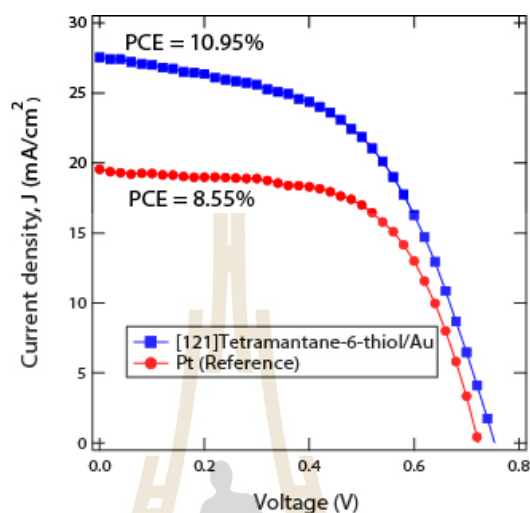


Figure 4.1 J-V curve and efficiency of [121]tetramantane-6-thiol on gold substrate (blue) and platinum reference (red) counter electrode.

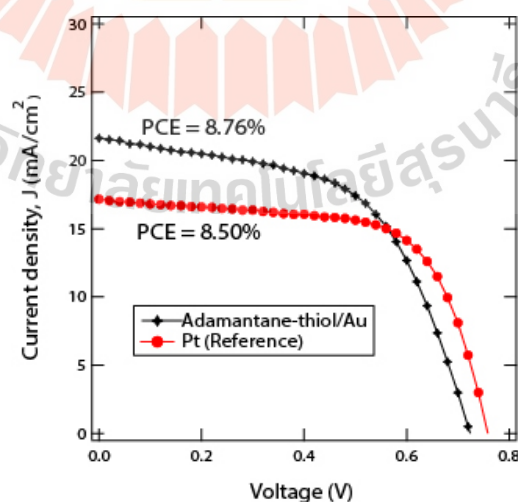


Figure 4.2 J-V curve and efficiency of adamantane-thiol on gold substrate (black) and platinum reference (red) counter electrode.

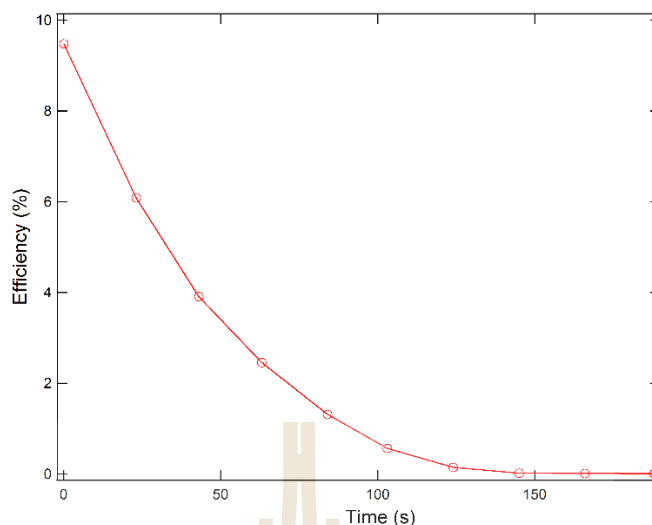


Figure 4.3 Decrease of DSSCs efficiency under destroying of iodine electrolyte.

4.2.2 Cobalt Electrolyte

There is a few way to solve stability problem such as replace electrolyte or media collector from iodine to another couple system, change the technique to deposit diamondoids films or change the substrate to other materials with strong resist corrosion in iodine electrolyte. Since, there are many redox couples with an ability to carry the electron, relaxation time of reaction must in order to electron generation time from dye-sensitizer and the energy level of reaction is close to Fermi level (E_F) of the counter electrode (see figure 4.4). As known iodine electrolyte is both good properties but very strong corrosion the electrode. Recently, cobalt redox couple was discovered and have both good properties, moreover, cobalt electrolyte is friendly with the gold electrode. This thesis also choosing cobalt electrolyte to study and solve the stability of diamondoids electrode in alternative electrolyte system. Cobalt electrolyte has different reaction energy from iodine electrolyte, so this not good for ruthenium complex dye-sensitizer. New dye-sensitizer generation was studied and found the Porphyrin-Based

Dye-Sensitizer is a good fit with cobalt electrolyte. This thesis choosing Y123 porphyrin-based dye-sensitizer with a different structure from the N719 dye (see figure 4.5) according to the previous study (Yum et al., 2012).

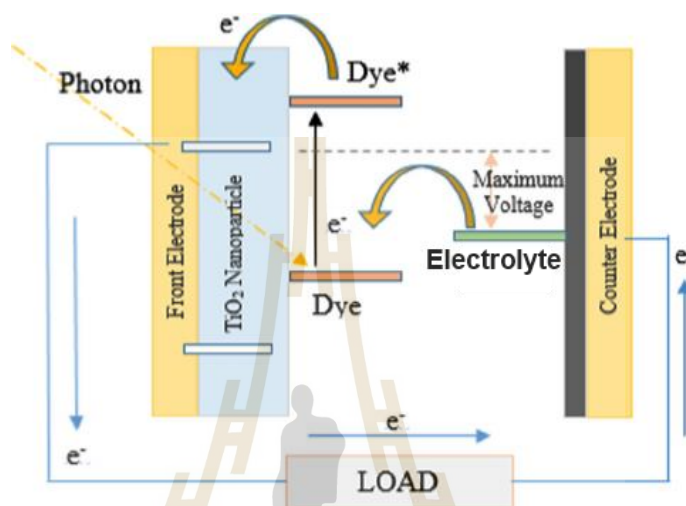


Figure 4.4 The DSSCs diagrams (Sugathan, 2015).

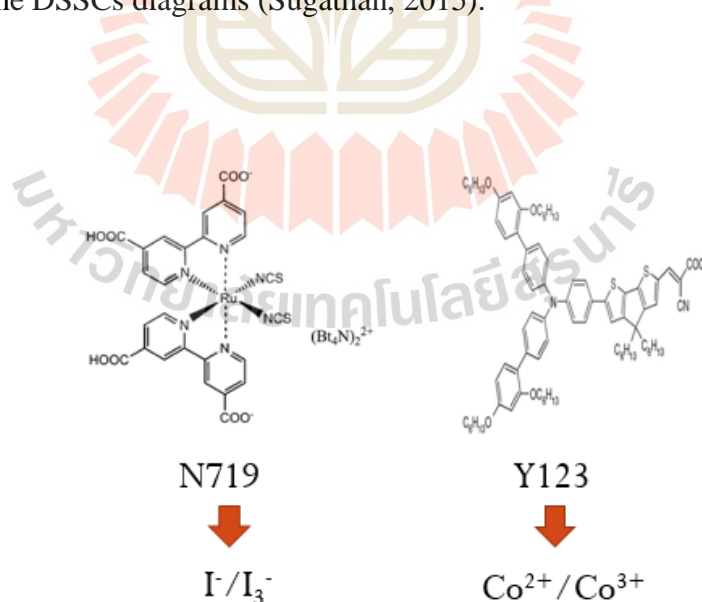


Figure 4.5 Structure of ruthenium-based dye-sensitizer (N719) and porphyrin-based dye-sensitizer (Y123).

The result from cobalt electrolyte was shown in figure 4.6, platinum and gold can use in this redox system with no corrosion. The short circuit current (J_{sc}) and open voltage (V_{oc}) from both electrodes are similar but fill factor of the gold electrode are better than the platinum electrode, the efficiency of Au electrode is 2.72% more than 2.22% of Pt electrode. Furthermore, the smallest molecule adamantane-thiol coated on the gold counter electrode is improved both of short circuit current (J_{sc}) and open circuit voltage (V_{oc}). The efficiency of diamondoids counter electrode is 3.90%, this improves more than 42.8% from gold substrate electrode. This result was confirmed diamondoids electrode can enhance the efficiency of the counter electrode in DSSCs. However, the efficiency of this technique is still low to comparing with standard Pt-iodine pairs, the other solution still necessary to study.

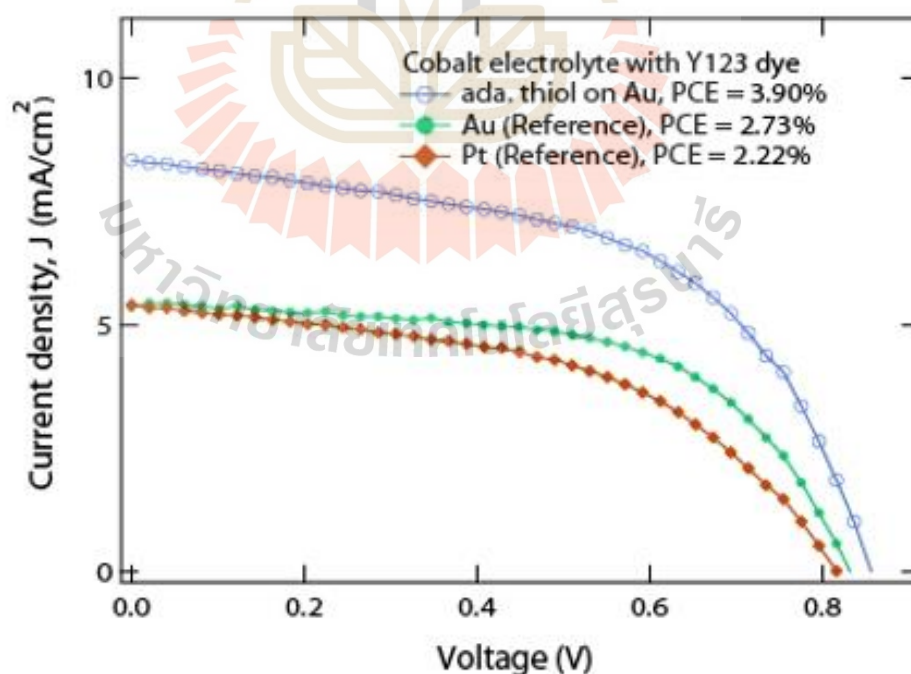


Figure 4.6 J-V curve and efficiency of DSSCs in cobalt electrolyte system.

4.2.3 CVD Films Counter Electrode

The thiol bonding is quite weak, it easy to destroy by iodine electrolyte. To make a stronger bonding, chemical vapor deposition (CVD) was choose by using adamantane powder as a precursor. Evaporate adamantane at 100 °C then flow to a high-temperature furnace (about 1050 °C), diamondoids will break the bond and reform on the surface of the substrate. The films of diamondoids were consists of SP³ bond (make strong films) and SP² bond (with help films conductive). By using CVD technique, we can growth diamondoid film on the sapphire substrate and reduce resistant to below one thousand ohms as shown in figure 4.7. After trying on a various substrate, the best counter electrode from CVD technique was found from the silicon substrate with strong films and good conductive. DSSCs from CVD-diamondoids electrode also give a high short-circuit current density (J_{sc}) as found from SAMs technique but the fill factor is quite low (see figure 4.8) may because of it still has a high series resistant (the effect of resistant to efficient of solar cells was explained in chapter III), the conductive properties will next discussing in section C_{1s} from XPS. The efficiency from CVD-diamondoids electrode is 6.26% comparing to 9.21% of platinum referent electrode, this electrode has a very good stability and proof the diamondoids films can use as the counter electrode for DSSCs. However, because of in difficult to growth films and low efficiency, diamondoids film from CVD technique still need to develop to find a better condition. Note: Diamondoids films from CVD technique has some interesting properties such as magnetic behavior and enhance the capacitance with not detailing in this thesis.

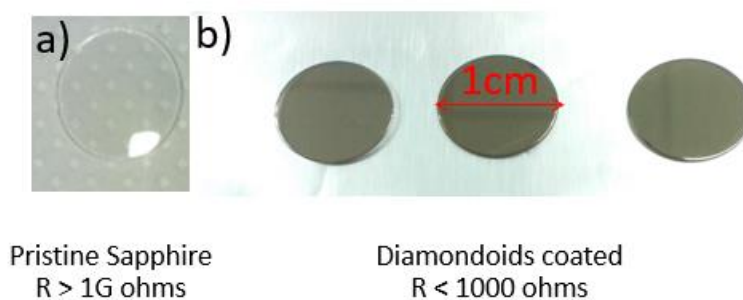


Figure 4.7 Carbon coated on sapphire substrate a)pristine sapphire and b)after coating with carbon from diamondoid.

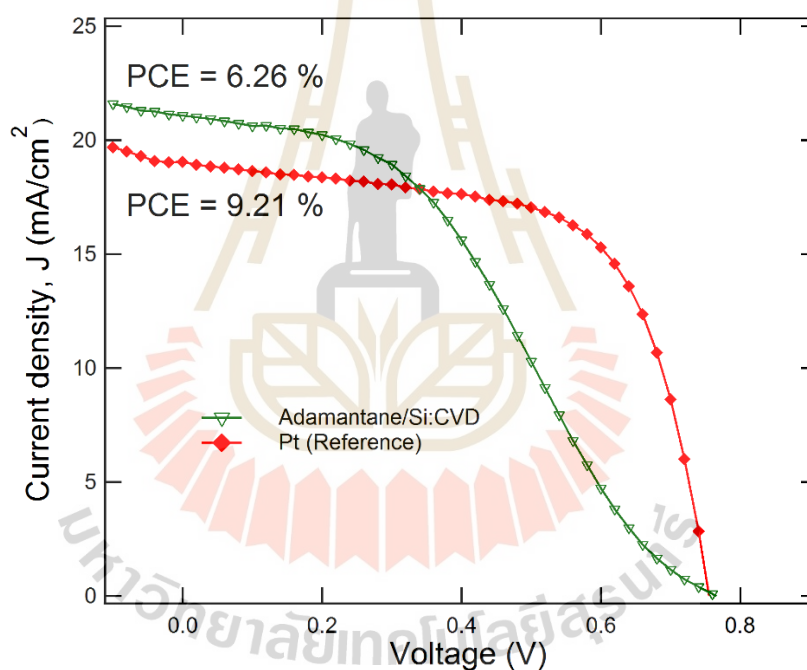


Figure 4.8 J-V curve and efficiency of DSSCs from CVD technique.

4.2.4 Platinum substrate counter electrode

As diamondoids counter electrode from SAMs technique on gold has a very high efficiency but low stability, on the other hand, diamondoids films from CVD technique and in cobalt electrolyte are good stable while still low efficient. The

platinum counter electrode was mentioned as the best efficient and good stability, even so, SAMs technique cannot direct growth diamondoids films on the platinum substrate because of non-matching of surface energy. In 2006, Petrovykh and co-worker were successful to study the Alkane-thiol on platinum by SAMs (Petrovykh et al., 2006). Alkane-thiol is like diamondoids-thiol, by replacing diamondoids with a linear chain of carbon. The key to contact the thiol function to the platinum substrate is to modify a surface of platinum by using Piranha solution (piranha solution consisting of 70% of H_2SO_4 and 30% of H_2O_2 , (vol/vol)). After immerse platinum in piranha solution for 15 mins follow with rinsed by isopropanol and DI water, the films were dried by nitrogen gas and immediately immersing in diamondoids-thiol solution (100 mg of diamondoids-thiol in 10ml of 9:1 toluene/ethyl alcohol, (vol/vol)). In adamantane-thiol solution, Pt substrate was immersed for 7 days but only 1 hour for a tetramantane-thiol solution because tetramantane-thiol has a stronger interaction with the substrate. The efficiency of diamondoids by SAMs technique on platinum substrate give a very good result as expected, first, the films have a very strong and stable in iodine electrolyte solution. As shown in figure 4.9, the tetramantane-thiol coated on Pt substrate (TET-T/Pt) have the short-circuit current density $J_{sc} = 21.03 \text{ mA/cm}^2$ higher than 18.65 mA/cm^2 of Pt reference electrode, both of it have a same open-circuit voltage (V_{oc}) at 0.72 volt. And the efficiency of TET-T/Pt is 9.43% comparing to 8.52% of Pt electrode, this improve more than 10% from Pt electrode. For a smaller molecule, Adamantane-thiol (ADA-T/Pt) has a similar result to TETT/Pt (see figure 4.10) with $J_{sc} = 20.8 \text{ mA/cm}^2$, it has a little bit higher of V_{oc} at 0.75 volt and 9.55% of efficiency.

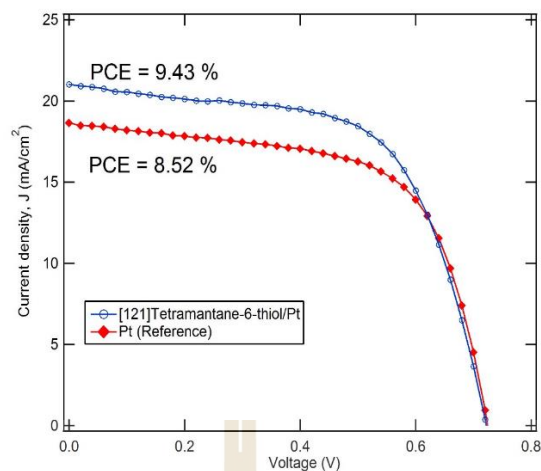


Figure 4.9 J-V curve and efficiency of [121]tetramantane-6-thiol on platinum substrate (blue) and platinum reference (red) counter electrode.

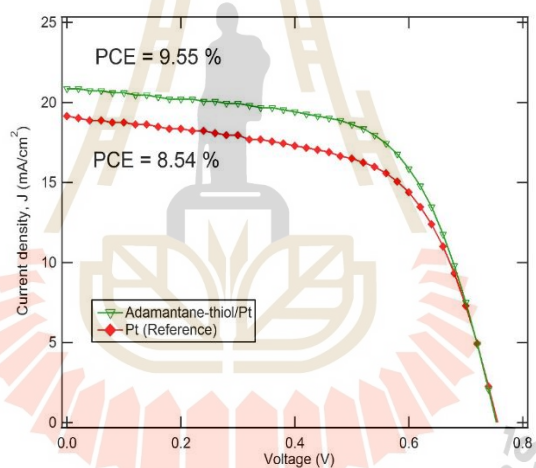


Figure 4.10 J-V curve and efficiency of adamantane-thiol on platinum substrate (green) and platinum reference (red) counter electrode.

4.3 Atomic Force Microscopy Result

After finding the enhancing of short circuit current (J_{sc}), the few characterizing technique was chosen for explain mechanism hereafter. The Atomic Force Microscopic (AFM) was used for investigating surface roughness from topology image as shown in figure 4.11, the surface roughness of adamantane-thiol on gold substrate a) is similar to

the surface roughness of platinum substrate b), indicated the enhance of efficiency and short circuit current not from the better porosity. figure 4.11c) shown a conductive mode of Atomic Force Microscopic (C-AFM), white regions represent the better electron flowing and homogeneous displacement of diamondoids films. Moreover, the tunneling current and apply voltage diagram shown non-ohmic characteristic and look like Resistive switching behaviors from the previous study (Nafe, 2013), this indicates diamondoids films can use as a resistive random-access memory as shown in figure 4.12.

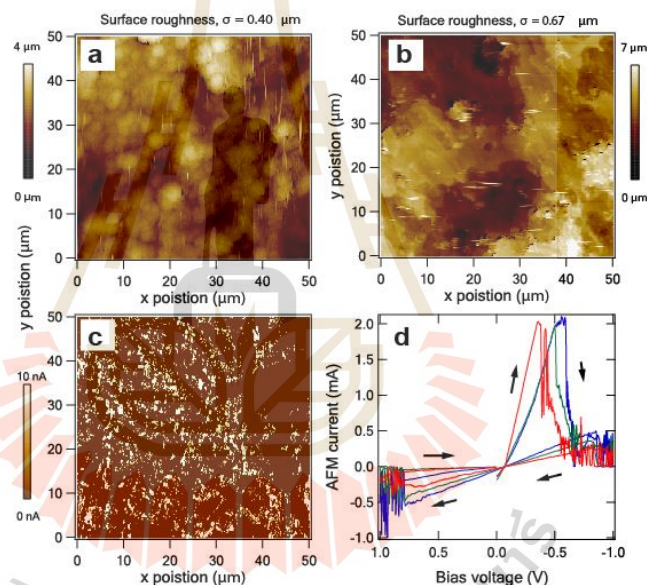


Figure 4.11 AFM images in topography mode of adamantane-thiol/sputtered Au/tungsten substrate a) and sputtered Pt/tungsten substrate b) with rough nesses (height standard deviation) of $0.40 \mu\text{m}$ and $0.67 \mu\text{m}$, respectively. c) the conductive mode AFM image of adamantane-thiol/Au/W in air with bias = -1 V ; the image shows that the electrons can transfer better in the white regions. d) the current vs. voltage curve of adamantane-thiol/Au/W at various points on the sample show the asymmetry between positive and negative bias, indicating that the electrons can transfer out of the substrate better than the other way around.

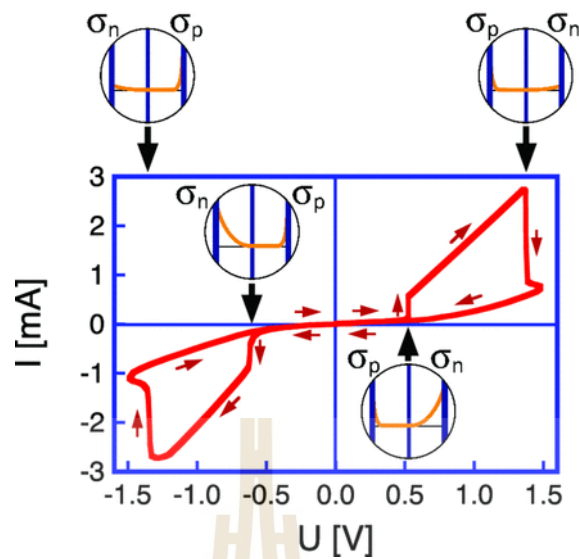


Figure 4.12 The resistive switching behavior shown looping character (Nafe, 2013).

4.4 Impedance Result

The result from AFM indicated, increasing efficiency in DSSCs not from extrinsic properties of the diamondoids films porosity. In this part is trying to explain the effective impedance to electron flow. The result from symmetrical electrode measurement setup (detailed in chapter III) shown in figure 4.13. After using the standard model of DSSCs symmetrical electrode [Nickel sulfide films with significantly enhanced electrochemical performance induced by self-assembly of 4-aminothiophenol and their application in dye-sensitized solar cells], the series resistance (R_s), charge transfer resistance (R_{ct}) and double layer capacitance (C_{dl}) were calculated as shown in table 4.1. The relation of R_s , R_{ct} , and C_{dl} would help to explain the mechanism of charge transfer at the counter electrode of DSSCs as Lim and co-worker was detailed (Lim et al., 2015). The Electron lifetime (t_n) is equal to $R_{ct} * C_{dl}$, this means if R_{ct} bigger is better for electrolyte to capture electron from counter electrode. The Transfer time (t_s) is time which electrolyte need to extract electron from

electrode equal to $R_s \cdot C_{dl}$, with lower is better. As seen in Table 4.1, R_s of diamondoids films on the platinum substrate is lower than platinum reference electrode, meaning electrolyte can receipt electron from diamondoids films easier. The R_{ct} of adamantane-thiol films is lower than Pt electrode but C_{dl} is bigger, calculated t_n from $R_{ct} \cdot C_{dl}$ of diamondoids films still higher than Pt electrode meaning recombination of electron in diamondoid is lower than Pt electrode. Moreover, tetramantane-thiol films give a higher both of R_{ct} and C_{dl} this brings tetramantane gain a clearly higher of efficient.

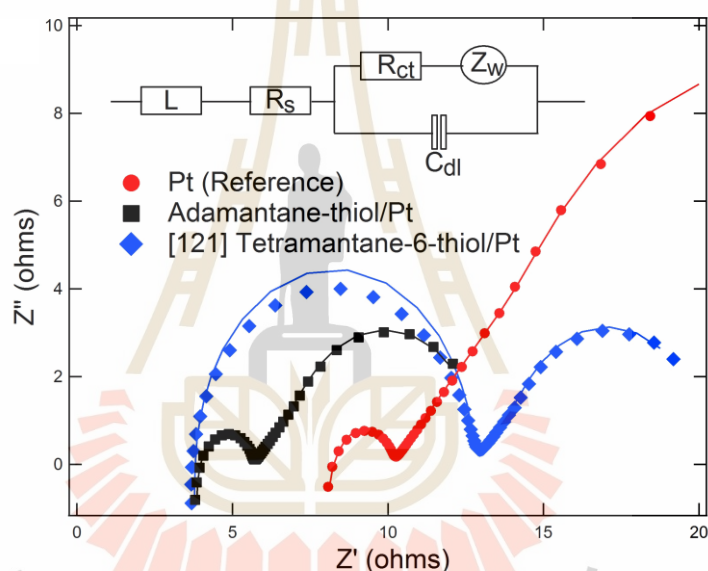


Figure 4.13 The result of impedance from Electrochemical Impedance Spectroscopy, point are the raw data and line are fitting curve of insect model.

Table 4.1 Fitting parameter of symmetrical standard models of DSSCs.

Electrode	R_s (Ω)	R_{ct} (Ω)	C_{dl} (μF)	t_s (μs)	t_n (μs)
Pt (Reference)	8.41	1.68	5.26	44.24	8.84
Adamantane-thiol/Pt	4.04	1.59	10.30	41.61	16.38
[121] Tetramantane-6-thiol/Pt	3.83	8.76	6.12	23.44	53.61

4.5 Cyclic Voltammetry Result

Because of electrolyte or hole transporting materials is in the liquid state, the cyclic voltammetry (CV) was chosen for study the reaction of the electrolyte. Cyclic voltammetry (CV) gave an information about reduction and oxidation state between the electrolyte and the electrode as shown in figure 4.14. The result showed that both of diamondoids electrode have a higher current density than the platinum electrode, this meaning there is more electron flowing through diamondoids electrode than Pt electrode. Moreover, reduction peak of electrolyte and TET-T/Pt large shifted to lower energy, would mean electrolyte use lower energy to extract an electron from the counter electrode. Information from the cyclic voltammetry (CV) was well supported to explain the improved efficiency of diamondoids counter electrode in DSSCs.

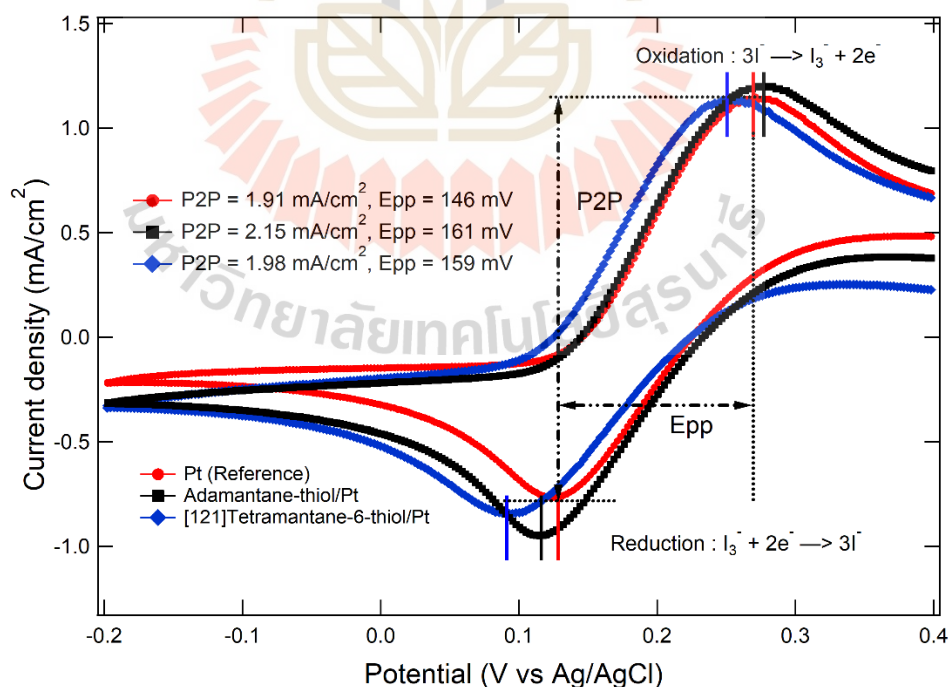


Figure 4.14 The result of cyclic voltammetry at a scan rate of 20 mV/s in 10mM LiI, 1mM I₂, and 0.1M LiClO₄ in an acetonitrile solution.

4.6 Photoemission Spectroscopy Result

The Electrical Impedance Spectroscopy (EIS) and the cyclic voltammetry (CV) gave the information of overall effect from diamondoids films to the electrolyte system but cannot explain the relation in the local electronic properties of diamondoids. The X-ray photoemission spectroscopy (XPS) was used for investigating the electronic structure and this information would help to align the energy level and explain mechanism in term of energy relation of diamondoids counter electrode and DSSCs system.

4.6.1 XPS Interpretation of Carbon C_{1s}

The previous section was mentioned in CVD-diamondoids consisting the mixed of SP² and SP³ -hybridization of carbon and the films is quite good conductive. In this part, the core level C_{1s} of carbon studied by XPS technique which can extract SP²/SP³ ratio by fitting the combination peak as shown in figure 4.15. The result shown CVD-diamondoids films consist of 81.19% of SP² with dominating conductive term, even so, this still poor conduct when comparing to the metal electrode and leading the fill factor of DSSCs quite low as mentioned in the efficiency section.

4.6.2 Work Function

In this part, the work function of the electrode was calculated by measured cut off and Fermi energy. The maximum kinetics energy is a value of a difference between cut off edge and Fermi energy, then using Einstein equation of photoelectric effect ($E_{k,maxim} = hv - \phi$) to calculate the work function as shown in figure 4.16. As the result shown in figure 4.17, diamondoids can expanding the state of cut off edge and

increasing the maximum kinetics energy. That means the work function of the electrode was reduced. The work functions were calculated and show in the inset of figure 4.17, the result showed the most reduced work function was found from tetramantane-thiol films on the platinum substrate and adamantane-thiol also reducing the work function, this information was supporting to explain the DSSCs efficiency result by alignment the energy level.

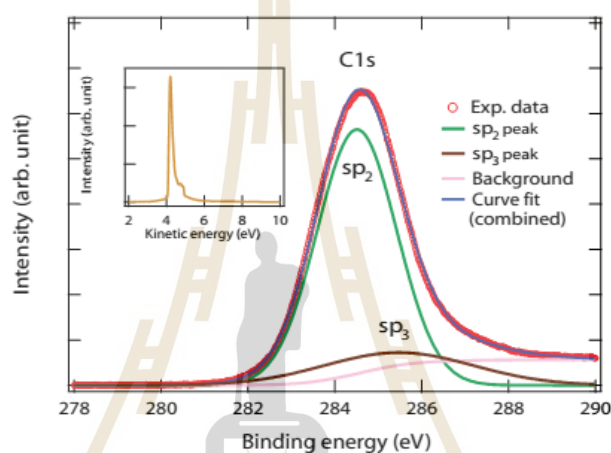


Figure 4.15 The result of C1s from the X-ray photoemission (XPS) data of the CVD ada. on Si substrate, measured at SLRI Beamline 3.2a, shows the carbon peaks of both sp₂ and sp₃ with the ratio of 81% and 19%, respectively.

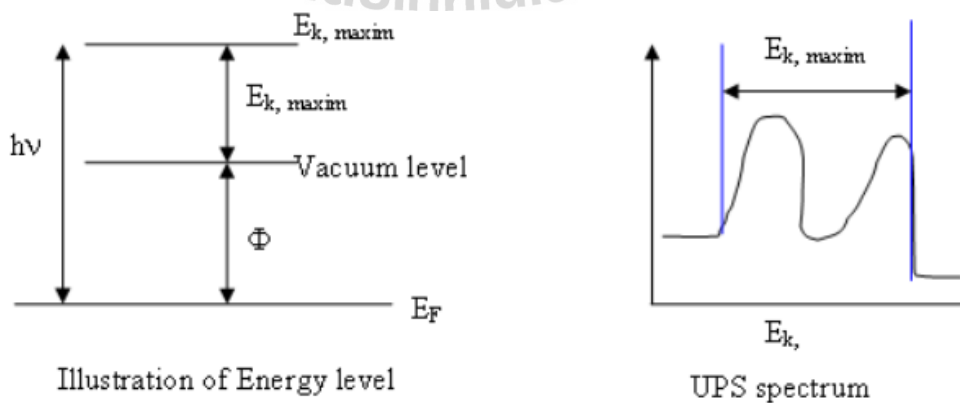


Figure 4.16 The work function can be calculated from Einstein relation.

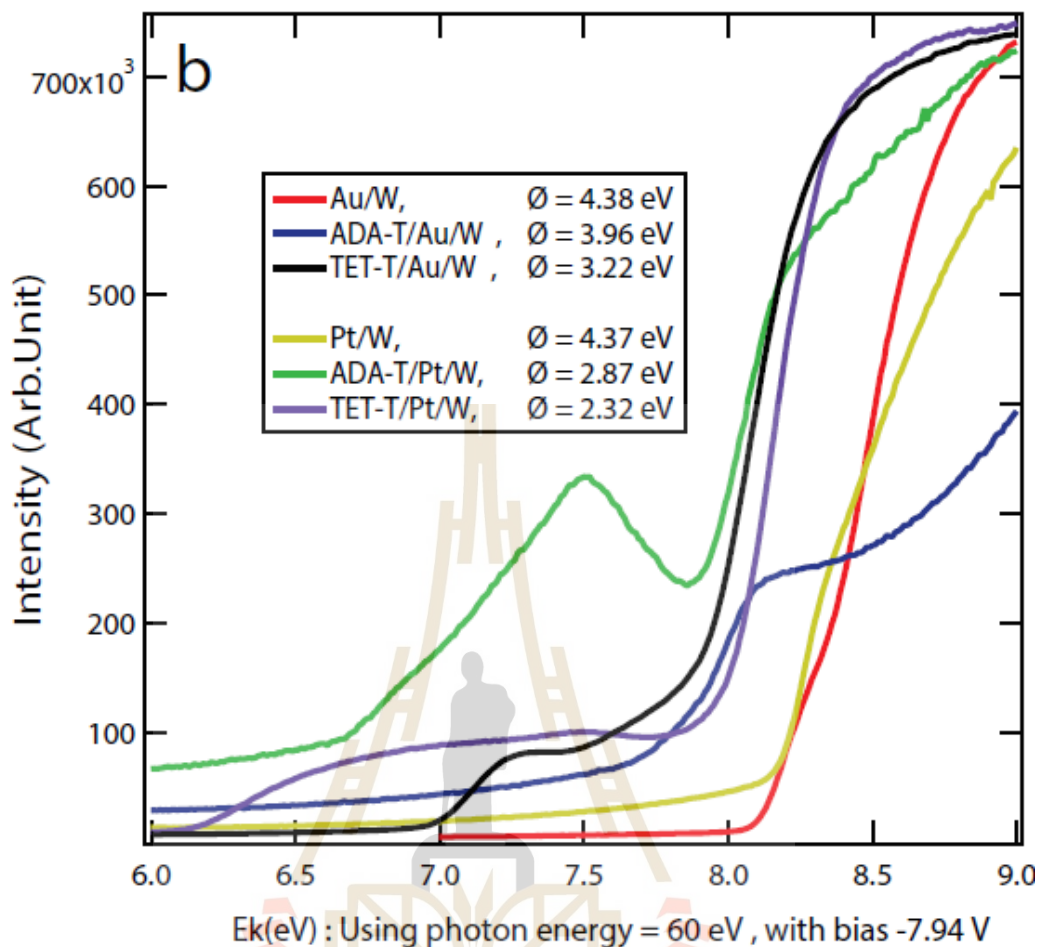


Figure 4.17 The cut off edge of diamondoids on gold and platinum substrate.

4.7 Energy Alignment

This is the final part to explain why diamondoids films can improve DSSCs efficient. After alignment energy level of DSSCs diagram according to previous studies (Eithiraj et al., 2013; Lelii et al., 2014; Liu et al., 2015), the Fermi level state of the platinum electrode is lower than reduction state of iodine electrolyte (see figure 4.18) because Pt has a high work function. Diamondoids films can reduce the work function of platinum or gold substrate and be leading the Fermi level state more closed to the reduction state of electrolyte this would make electrolyte easier to pick electron up from

the counter electrode. The shifting to lower energy of reduction peak of diamondoids films from cyclic voltammetry (CV) would be from this behavior and make the better efficient in DSSCs.

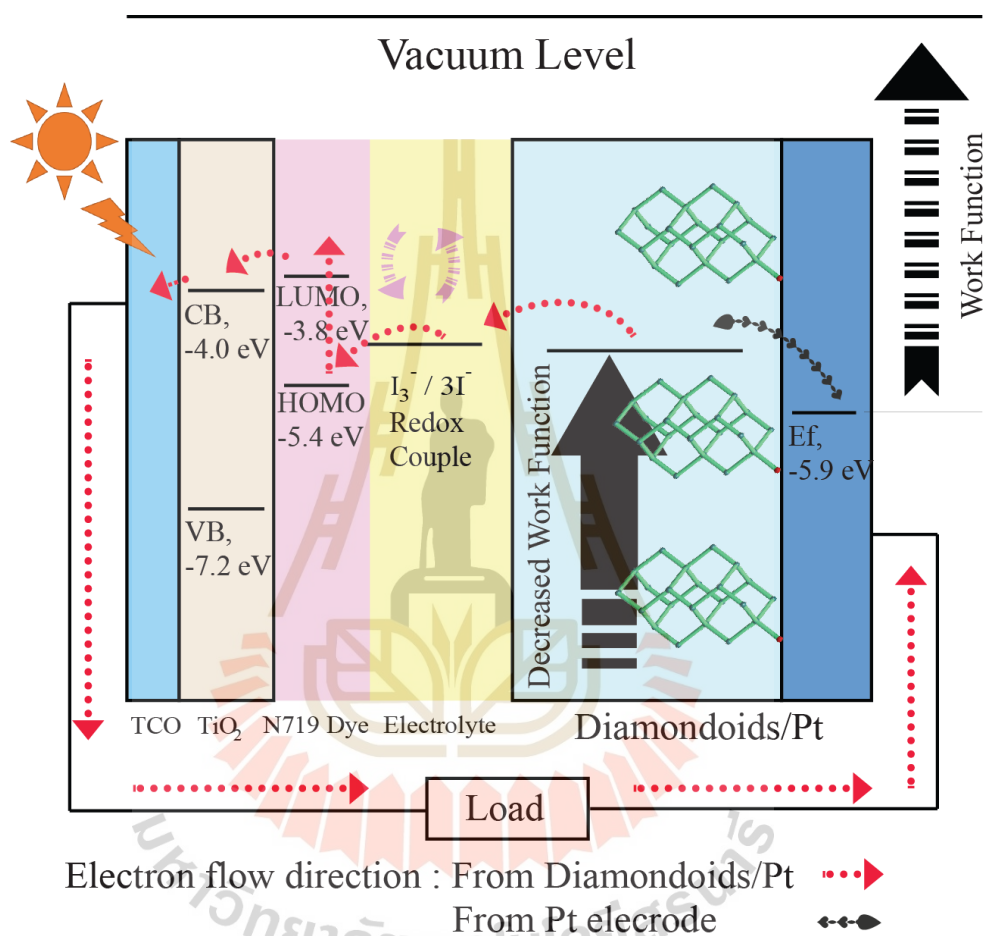


Figure 4.18 Energy alignment of DSSCs.

4.8 Summary

All this chapter is trying to explain why diamondoids film can enhance the efficiency of DSSCs. The result shown diamondoids films on the gold substrate via SAMs technique can improve the efficiency of DSSCs but very poor stability. To solve the problem new electrolyte, cobalt electrolyte was replaced iodine electrolyte and give

the result in the same way with a good stability but not much efficiency. The diamondoids film from CVD technique was tried, very strong stability and high short-circuits current were found but low fill factor because of a higher of series resistant of the electrode. Diamondoids films on the platinum substrate via SAMs is the best solution, given both of higher efficiency and good stability. The explaining start from the surface rashness of diamondoids is nearly of platinum films indicated enhancing not from porosity effect. Impedance result shown diamondoids film on Pt has lower series resistant (R_s) and leading to lower in the transfer time (t_n), the higher of charge transfer resistant (R_{ct}) leading to better in electron lifetime (t_n) that can protect the recombination of electron and hole. The result from CV shown higher electron flow from diamondoids films and shifting of reduction peak with supported from reduced of the work function of diamondoids films. This thesis has shown only two metal substrates for SAMs, however other metal was trying and test, but it does not work. For both iodine and cobalt electrolyte, platinum and gold are suitable because matching of work function so good metal substrate should have work function nearly 5.1-5.6 eV, another metal work function is shown in Table 4.2.

Table 4.2 Work function of metals (Tipler and Llewellyn, 1999).

Element	W (eV)						
Ag	4.26	Al	4.28	As	3.75	Au	5.10
B	4.45	Ba	2.70	Be	4.98	Bi	4.22
C	5.00	Ca	2.87	Cd	4.22	Ce	2.90
Co	5.00	Cr	4.50	Cs	2.14	Cu	4.65
Eu	2.50	Fe	4.50	Ga	4.20	Gd	3.10
Hf	3.90	Hg	4.49	In	4.12	Ir	5.27
K	2.30	La	3.50	Li	2.90	Lu	3.30
Mg	3.66	Mn	4.10	Mo	4.60	Na	2.75
Nb	4.30	Nd	3.20	Ni	5.15	Os	4.83
Pb	4.25	Pt	5.65	Rb	2.16	Re	4.96
Rh	4.98	Ru	4.71	Sb	4.55	Sc	3.50
Se	5.90	Si	4.85	Sm	2.70	Sn	4.42
Sr	2.59	Ta	4.25	Tb	3.00	Te	4.95
Th	3.40	Ti	4.33	Tl	3.84	U	3.63
V	4.30	W	4.55	Y	3.10	Zn	4.33
Zr	4.05						

CHAPTER V

CONCLUSION AND RECOMMENDATION

5.1 Conclusion of Thesis

Dye-sensitized solar cells (DSSCs), the new type of solar cells was expected to replace silicon and thin films solar cells. Even though DSSCs are easy to produce, low cost, low weight, flexible and environmentally friendly, the efficiency and stability of DSSCs not yet good enough to be produced for sale. Platinum was a candidate the best counter electrode of DSSCs with the highest efficiency and good stability, but platinum is still expensive, alternative counter electrode or improves efficient from the platinum electrode is necessary to reduce cost per energy conversion. This thesis was interested in diamondoids (the nanostructure of diamond), the strange in electronic properties such as can emitted electron by itself and reducing the work function of an electrode may help to improve the efficiency of DSSCs. By using the simple self-assembled monolayers (SAMs) technique, diamondoids can deposit of gold substrate by bonding of thiol function and can enhance the efficiency of DSSCs from the standard platinum electrode by 28%. However, diamondoids on the gold substrate are quickly down because of destroying of iodine electrolyte to the gold substrate. Diamondoids films coated on silicon substrate via CVD technique and other cobalt electrolyte were tried and can solve stability problem and can enhance the current from reference substrate but the efficiency is not good enough. Back to the simple, diamondoids films was succeeded to deposit on the platinum substrate by modifying the surface of platinum

with piranha solution (70% of H_2SO_4 : 30% of H_2O_2 , (vol/vol)) before using SAMs technique. The diamondoids on Pt electrodes are good both of efficiency and stability. To explain how diamondoids can enhance the efficiency of DSSCs, Electrochemical Impedance Spectroscopy (EIS) and Cyclic Voltammetry (CV) were used for studying the global properties of interaction between diamondoid films and electrolyte. Impedance result shown diamondoids film on Pt has low series resistance (R_s) than Pt and leading to lower in the transfer time (t_n), the high charge transfer resistance (R_{ct}) leading to better in electron lifetime (t_n) that can protect the recombination of electron and hole. The result from CV shown higher electron flow from diamondoids films and shifting of reduction peak with supported from reduced of the work function of diamondoids films. As mentioned in Chapter II, Narasimha, and coworker (Narasimha et al., 2015) discovered diamondoids monolayer can reduce the surface work function of the gold substrate. In that work, they explained how diamondoids reduce the work function of metal electrode by ionized radical cation charge on Au surface (see Figure 5.1). Diamondoid must remove an electron to form charge radical cation on the surface. The relative positive charge of diamondoid will attract electron of the substrate and be helping substrate easier to release the electron. This meaning the work function of metal substrate was reduced (because electron needs less energy to leave from metal surface).

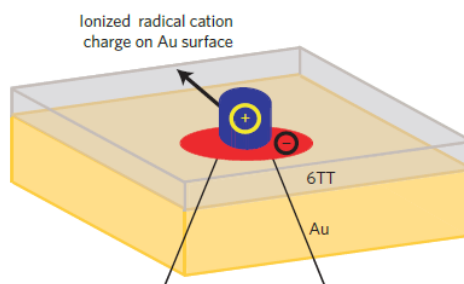
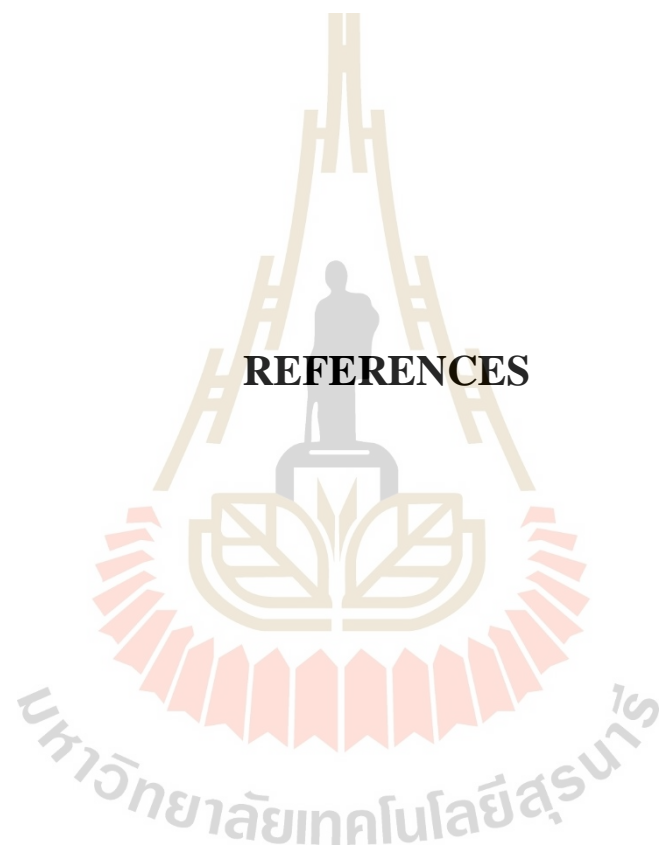


Figure 5.1 Schematic of the cation-based model of diamondoids on Au substrate (Narasimha, 2015).

5.2 Recommendation and Future Direction

Even though, DSSCs have a lot of benefit and aspect to solve energy crisis problem, one of critical drawback is DSSCs using a liquid electrolyte with not good in the long term. The problems were from liquid electrolyte can leak from the cells leading the efficient of DSSCs was reduced in a few of month and another reason is liquid electrolyte is unstable and destroy dye molecule. To solve the problem, a solid electrolyte was studied and the structure of DSSCs was change. As detailed in chapter 4, the electrolyte must be matching with the energy level of dye-sensitizer, in the same way, the sensitizer has been changed according to the electrolyte. The new solid electrolyte is call hole transporting materials (HTMs), and some materials in perovskite are matching energy to use as the sensitizer. A new type replaced DSSCs was called Perovskite solar cells, with good efficient (21%) and longer stability (more than 1 year). Perovskite solar cells were aspect to solve the problem which DSSCs cannot actualize. However, diamondoids still interested by added to the layer between the hole transporting layer and back contact of perovskite solar cell, diamondoids layer would enhance the efficiency of perovskite solar cells as present on DSSCs.

REFERENCES



REFERENCES

- Balaban, A.T., and Schleyer, P.V.R. (1978). Systematic classification and nomenclature of diamond hydrocarbons. 1. Graph-theoretical enumeration of polymantanes. **Tetrahedron**. 34: 3599.
- Bostedt, C., Van Buuren, T., Willey, T.M., Franco, N., Terminello, L.J., Heske, C., and Miller T. (2004). Strong quantum-confinement effects in the conduction band of germanium nanocrystals. **Applied physics letters**. 84(20): 4056-4058.
- Cupas, C., von R. Schleyer, P., and Trecker D.J. (1965). Congressane. **Journal of the American Chemical Society**. 87(4): 917-918.
- Dahl, J.E., Liu, S.G., and Carlson, R.M.K. (2003). Isolation and structure of higher diamondoids, Nanometer-Sized diamond molecules. **Science**. 299: 96.
- Eithiraj, R.D., and Geethalakshmi, K.R. (2013). Suitability of amorphous TiO₂ nanoparticles as a photoelectrode in dye sensitized solar cells: A DFTTDDFT study. **Chemical Physics Letters**. 585: 138-142.
- Hala, S., Landa, S., and Hanu, V. (1966). Isolation of Tetracyclo [6.3. 1.02, 6.05, 10] dodecane and Pentacyclo [7.3. 1.1. 4, 12.02, 7.06, 11] tetradecane (Diamantane) from Petroleum. **Angewandte Chemie International Edition**. 5(12): 1045-1046.
- Hernadi, K., Fonseca, A., Nagy, J.B., Bernaerts, D., and Lucas, A.A. (1996). Fe-catalyzed carbon nanotube formation. **Carbon**. 34: 1249.

- Hoover, R. (2014). Need to track organic nano-particles across the Universe? NASA's Got an App for That. **NASA**. 02: 22.
- Hwang, S., Moon, J., Lee, S., Kim, D.-H., Choi, W., and Jeon, M. (2007). Carbon nanotubes as counter electrode for dye-sensitized solar cells. **Electron Letter**. 43: 1455.
- Imoto, K., Takahashi, K., Yamaguchi, T., Komura, T., Nakamura, J., and Murata, K. (2003). High-performance carbon counter electrode for dye-sensitized solar cells. **Solar Energy Materials and Solar Cells**. 79: 459-469.
- Kim, H.S., Ko, S.B., Jang, I.H., and Park, N.G. (2011). Improvement of mass transport of the [Co(bpy)₃] II/III redox couple by controlling nanostructure of TiO₂ films in dye-sensitized solar cells. **Chemical Communications**. 47(47): 12637-12639.
- Kojima, A., Teshima, K., Shirai, Y., and Miyasaka, T. (2009). Organometal halide perovskites as visible-light sensitizers for photovoltaic cells. **Journal of the American Chemical Society**. 131(17): 6050-6051.
- Landa, S., and Machacek, V. (1933). Adamantane, a new hydrocarbon extracted from petroleum. **Collection of Czechoslovak Chemical Communications**. 5: 1-5.
- Landt, L., Klunder, K., Willey, T.M., van Buuren, T., Dahl, J.E., Carlson, R.M.K., Moller, T., and Bostedt, C. (2010). In preparation of the influence of a single thiol group on the electronic and optical properties of the smallest diamondoid adamantane. **The Journal of Chemical Physics**. 132: 024710.
- LaRue, J.L., White, J.D., Nahler, N.H., Liu, Z., Sun, Y., Pianetta, P.A., and Wodtke, A.M. (2008). The work function of submonolayer cesium-covered gold: A photoelectron spectroscopy study. **The Journal of chemical physics**. 129(2): 024709.

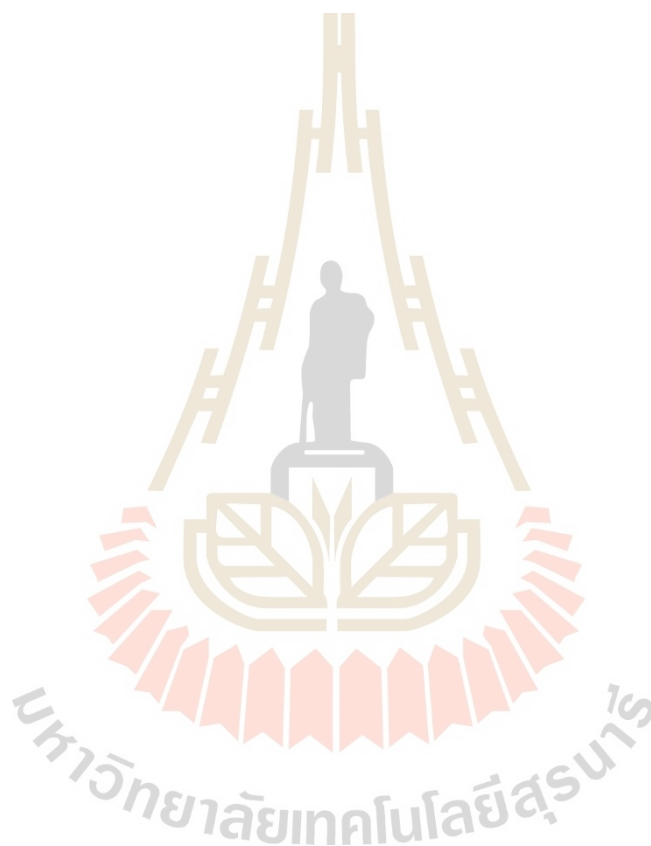
- Lee, W.-J., Ramasamy, E., Lee, D.-Y., Min, B.-K., and Song, J.-S. (2006). Dye-sensitized solar cells with spray-coated CNT counter electrode. *Proc. International Society for Optics and Photonics*. 6038: 60381T.
- Lelii, C., Bawendi, M.G., Biagini, P., Chen P.Y., Crucianelli, M., D'Arcy, J.M., and Po, R. (2014). Enhanced photovoltaic performance with co-sensitization of quantum dots and an organic dye in dye-sensitized solar cells. *Journal of Materials Chemistry A*. 2(43): 18375-18382.
- Lenzke, K. (2006). Photoionisation von molekularen Diamanten. **Diplomarbeit**. Berlin.
- Lim, S.P., Pandikumar, A., Lim, H.N., Ramaraj, R., and Huang, N.M. (2015). Boosting photovoltaic performance of dye-sensitized solar cells using silver nanoparticle-decorated N, S-Co-doped-TiO₂ photoanode. *Scientific reports*. 5: 11922.
- Liu, X., Zhao, W., Cui, H., Xie, Y.A., Wang, Y., Xu, T., and Huang, F. (2015). Organic inorganic halide perovskite based solar cells revolutionary progress in photovoltaics. *Inorganic Chemistry Frontiers*. 2(4): 315-335.
- McKervey, M.A. (1980). Synthetic Approaches to Large Diamondoid Hydrocarbons. *Tetrahedron*. 36: 971.
- Meevasana, W., Supruangnet, R., Nakajima, H., Topon, O., Amornkitbamrung, V., and Songsiriritthigul, P. (2009). Electron affinity study of adamantane on Si(111). *Applied Surface Science*. 256: 934.
- Nafe, H. (2013). Resistive Switching: A Solid-State Electrochemical Phenomenon. *ECS Journal of Solid State Science and Technology*. 2(11): P423-P431.
- Narasimha, K.T., Ge, C., Fabbri, J.D., Clay, W., Tkachenko, B.A., Fokin, A.A., Schreiner, P.R., Dahl, J.E., Carlson, R.M.K., Shen, Z.X., and Melosh, N.A.

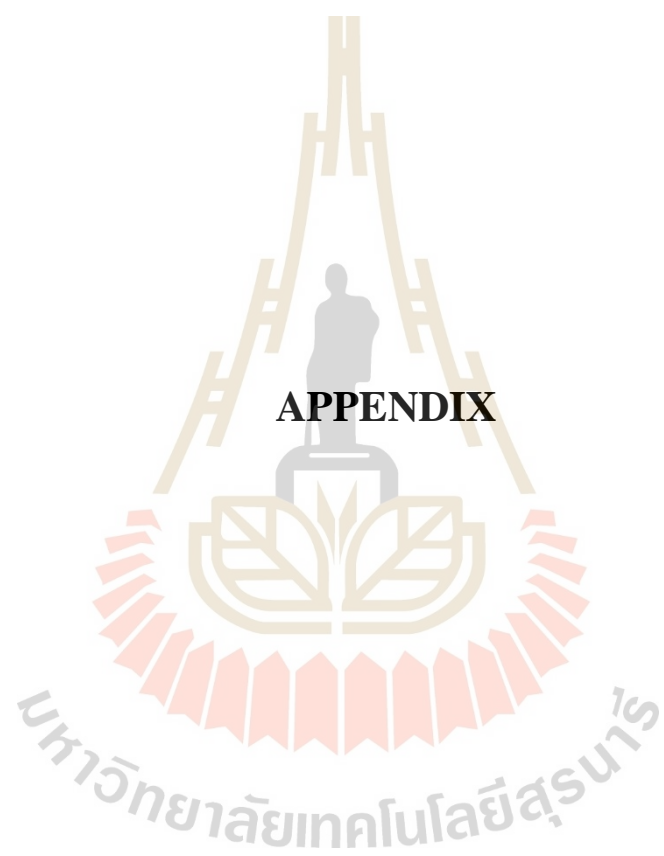
- (2016). Ultralow effective work function surfaces using diamondoid monolayers. **Nature Nanotechnology**. 11: 267272.
- O'Regan, B., and Grätzel, M. (1991). A low-cost, high-efficiency solar cell based on dye-sensitized colloidal TiO₂ films. **Nature**. 353(6346): 737740.
- Pessoa, R.S., Fraga, M.A., Santos, L.V., Galvo, N.K.A.M., Maciel, H.S., and Massi, M. (2014). Plasma-assisted techniques for growing hard nanostructured coatings: An overview." *Anti-Abrasive Nanocoatings*. **Woodhead Publishing**. 455.
- Petrovykh, D.Y., Kimura-Suda, H., Opdahl, A., Richter, L.J., Tarlov, M.J., and Whitman, L.J. (2006). Alkanethiols on platinum: multicomponent self-assembled monolayers. **Langmuir**. 22(6): 2578-2587.
- Prelog, V., and Seiwert, R. (1941). "Über die synthese des adamantans. **Berichte der deutschen chemischen Gesellschaft (A and B Series)**. 74(10): 1644-1648.
- Saekow, S., Maiakree, W., Jarernboon, W., Pimanpang, S., and Amornkitbamrung, V. (2012). High intensity UV radiation ozone treatment of nanocrystalline TiO₂ layers for high efficiency of dye-sensitized solar cells. **Journal of NonCrystalline Solids**. 358: 2496-2500.
- Schleyer, P.V.R. (1957). A simple preparation of adamantane. **Journal of the American Chemical Society**. 79: 3202.
- Siroroj, S., Pimanpang, S., Towannang, M., Maiakree, W., Phumying, S., Jarernboon, W., and Amornkitbamrung, V. (2012). High performance dye-sensitized solar cell based on hydrothermally deposited multiwall carbon nanotube counter electrode. **Applied Physics Letters**. 100: 243303.

- Sugathan, V., John, E., and Sudhakar, K. (2015). Recent improvements in dye sensitized solar cells: A review. **Renewable and Sustainable Energy Reviews**. 52: 54-64.
- Tipler, P.A., and Llewellyn, R.A. (1999). Modern Physics, 3rd Ed. **W.H. Freeman**.
- Van Buuren, T., Dinh, L.N., Chase, L.L., Siekhaus, W.J., and Terminello, L.J. (1998). Changes in the electronic properties of Si nanocrystals as a function of particle size. **Physical Review Letters**. 80(17): 3803.
- Velten, J., Mozer, A.J., Li, D., Officer, D.L., Wallace, G.G., Baughman, R.H., and Zakhidov, A. (2012). Carbon nanotube/graphene nanocomposite as efficient counter electrodes in dye-sensitized solar cells. **Nanotechnology**. 23: 8.
- Willey, T.M., Bostedt, C., van Buuren, T., Dahl, J.E., Liu, S.G., Carlson, R.M.K., Terminello, L.J., and Möller, T. (2005). Molecular limits to the quantum confinement model in diamond clusters. **Physical Review Letters**. 95: 113401.
- Williams Jr, V.Z., von Ragu Schleyer, P., Gleicher, G.J., and Rodewald L.B. (1966). Triamantane. **Journal of the American Chemical Society**. 88(16): 3862-3863.
- Wingert, W.S. (1992). GC-MS analysis of diamondoid hydrocarbons in Smackover petroleum. **Fuel**. 71(1): 37-43.
- Yang, W.L., Fabbri1, J.D., Willey, T.M., Lee, J.R.I., Dahl, J.E., Carlson, R.M.K., Schreiner, P.R., Fokin, A.A., Tkachenko, B.A., Fokina, N.A., Meevasana, W., Mannella, N., Tanaka, K., Zhou, X.J., Buuren, T.V., Kelly, M.A., Hussain, Z., Melosh, N.A., and Shen, Z.-X. (2007). Monochromatic electron photoemission from diamondoid monolayers. **Science**. 316: 5830.
- Yue, G., Li, F., Tan, F., Li, G., Chen, C., and Wu, J. (2014). Nickel sulfide films with significantly enhanced electrochemical performance induced by self-assembly of

4-aminothiophenol and their application in dye-sensitized solar cells. **RSC Advances**. 4(109): 64068-64074.

Yum, J.-H., Baranoff, E., Kessler, F., Moehl, T., Ahmad, S., Bessho, T., and Grätzel, M. (2012). A cobalt complex redox shuttle for dye-sensitized solar cells with high open-circuit potentials. **Nature Communications**. 3: 631.





APPENDIX

APPENDIX

NEGATIVE ELECTRON AFFINITY (NEA) OF DIAMONDOIDS

In the beginning, this work was interested in a diamond phase of carbon. Because diamond has a strange property except for a very strong material. Diamond can be electron source of many application (e.g. for scanning electron microscope, X-ray tube) because it easy to emit an electron. However, diamond is very expensive material, diamondoids are nano sized of diamond which still retains that property and much cheaper than bulk diamond. Photoemission technique was chosen to study electron emitting from diamondoids. The photoemission spectroscopy can give a lot of information about the electronic structure of materials especially Fermi level (E_F) and secondary electron edge (cut off). The cut off is regions at the low kinetic energy of photoelectron, the normal cut off is according to the Fermi distribution equation. However, as mentioned in chapter II, diamondoids has a negative electron affinity properties (NEA) with can emits electron by itself (if has excited the electron in conduction band). The emitted electron has a low kinetic energy (few meV) and will present at low kinetic energy regions, this will show a sharp peak at cut off as shown in figure A.1. Because the limit of detector it cannot actual to measure the electron at few electron volt from zero kinetic energy, external potentials applied to bias the sample to shift peak to higher kinetic energy and this ability to measure the correct cutoff.

As shown in figure A.2, adamantane-thiol films on the gold substrate have a very high and sharp peak at a cut-off region with different from normal materials could confirm our diamondoids films has a negative electron affinity properties (NEA) and this may use in other application beyond enhancing the efficiency of DSSCs.

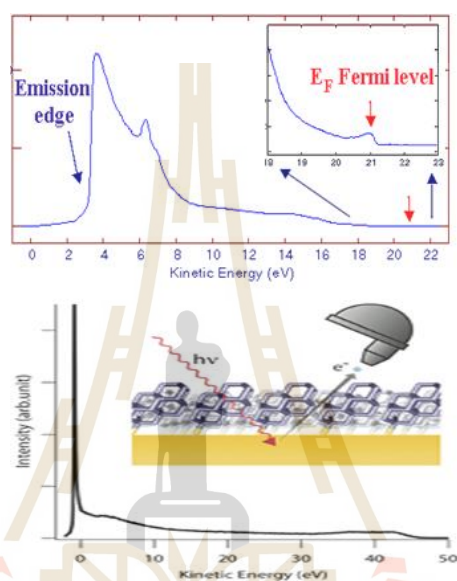


Figure A.1 Cut off region from normal materials and from diamondoids.

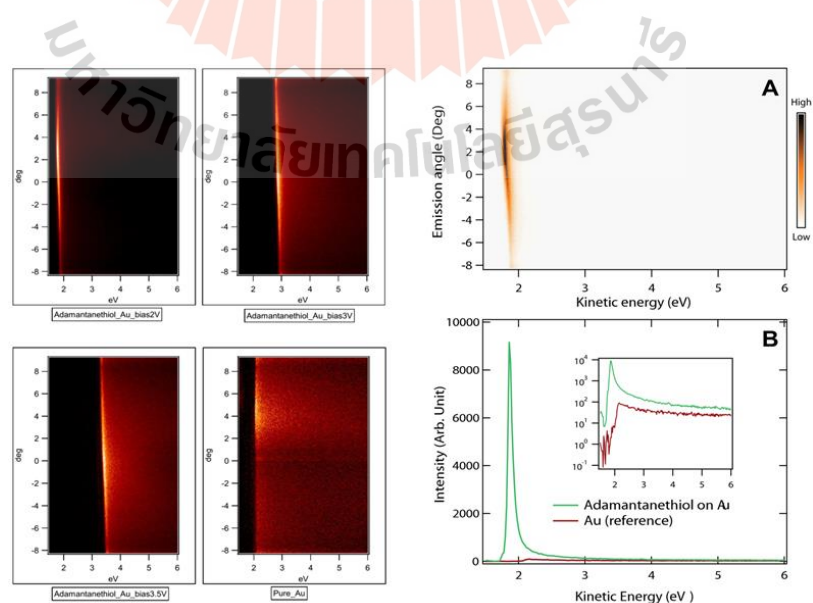


Figure A.2 The cut off from diamondoid films show the NEA behavior.

CURRICULUM VITAE

Name Mr. Sumeth Siriroj

Date of birth March 27, 1986

Place of birth 67 Sador village, Thumbol Jarapat, Sikhoraphum District, Surin
32110, Thailand

E-MAIL sumeth.siriroj@gmail.com

Education

Academic year

2005 - 2010 Chiang Mai University, Chiang Mai, Thailand
Bachelor of Science (Physics)

2010 - 2012 Khon Kaen University, Khon Kaen, Thailand
Master of Science (Material Science and Nanotechnology)

2012 - 2017 Suranaree University of Technology,
Nakhon Ratchasima, Thailand.
Doctor of Philosophy (Physics)

